Design of a Novel Electromechanical Gastric Resident Device for Long Term Controlled Drug Delivery

by

Ryan Koeppen

Submitted to the
Department of Mechanical Engineering
in Partial Fulfillment of the Requirements for the Degree of

Bachelor of Science in Mechanical Engineering

at the

Massachusetts Institute of Technology

June 2019

Signature of Author: _____

Department of Mechanical Engineering
May 10, 2019

Certified by: _____

Giovanni Traverso
Professor of Mechanical Engineering
Thesis Supervisor

Accepted by: _____

Maria Yang, PhD
Professor of Mechanical Engineering
Undergraduate Officer

Design of a Novel Electromechanical Gastric Resident Device for Long Term Controlled Drug Delivery

by

Ryan Koeppen

Submitted to the Department of Mechanical Engineering
on May 10, 2019 in Partial Fulfillment of the
Requirements for the Degree of

Bachelor of Science in Mechanical Engineering

ABSTRACT

Medication non-adherence is a global problem in health which has drastically hindered efforts to eradicate widespread diseases such as tuberculosis. Non-adherence has adverse effects on treatment efficacy and in the area of infectious disease it can increase the likelihood of developing antibiotic resistance to treatments. Despite global intervention efforts, non-adherence persists because the burden of administering medication is often placed directly on patients. One proposed strategy for overcoming non-adherence is the use of gastric resident devices, which are devices that hold large doses (~10-100 grams) of medication and deliver the medication in a controlled manner over long time periods (on the order of a month). Most gastric resident devices developed to date do not have the ability to load large doses of medication and release the pills in a controlled, pulsatile manner. Instead, they rely on continuous release processes which may not be sufficient for many treatments. This thesis details the design of a gastric resident device which can load approximately one week of medication and release the medication at a frequency of one pill per day using an electromechanically-driven mechanism. The device contains onboard electronics and a miniature direct current (DC) motor to drive a linkage that creates a reciprocating, linear motion at the output link. Intermediate, proof-of-concept tests were conducted to validate material choice, mechanism functionality, and mechanism reliability. A bench level prototype was developed and demonstrated the ability to release six pills from the action of controlled, electrical triggering only. Future work is being done to incorporate retention capabilities and self-contained electronics to make the device safe and autonomous for in vivo testing.

Thesis Supervisors: Giovanni Traverso; Robert Langer
Titles: Visiting Scientist, Assistant Professor of Mechanical Engineering;
David H. Koch Institute Professor of Chemical and Biomedical Engineering

Acknowledgements

I have a number of people to thank for their contributions to this project. Without their input and expertise, I would not have been able to bring this research to the place it is now. I want to thank Prof. Gio Traverso, Prof. Bob Langer, and Prof. Doug Hart for their mentorship, encouragement, and support as I developed this project. Thanks to Prof. Niclas Roxhed for his expertise and collaboration with electronics. Thanks to Malvika Verma, my graduate student supervisor, for providing me the opportunity to work on this project and for providing support and mentorship throughout the process of developing it. Thanks to John Salama, Talha Faiz, and Sope Eweje for providing support manufacturing and testing support the lab and helping disperse the workload of the project. Thanks to Tiffany Hua, Adam Declan Gwynne, Adam Wentworth, and Jake Weiner for their technical support with equipment, mechanical engineering expertise, and for brainstorming with me as the project progressed. Finally, thanks to Rebecca McManus for her technical electrical engineering expertise and support with prototyping electronics for the project.

Table of Contents

List of Figures

List of Tables

1. Introduction

1.1 Clinical Motivation

Medication Nonadherence

One major challenge in global health is medication non-adherence, when patients do not adhere exactly to the instructions given to them for their medicinal treatments. Many studies have demonstrated its validity, widespread occurrence, and effects on patients' treatment regimens. According to the WHO, the proportion of patients in developed countries who adhere to treatment for chronic illness averages near 50% [1]. This proportion may be even lower in developing countries; estimates for hypertension treatment in the Gambia and Seychelles place levels of adherence at only 27% and 26%, respectively [1]. It is also common for treatment non-adherence to transition to a complete discontinuation of medication regimens, often called "lost to follow up" [2,3]. The problem of medication non-adherence is further complicated by the fact that lack of adherence can be both deliberate and inadvertent. Because some treatments involve combinations of drugs with medication schedules that may be difficult to follow, treatment complexity has an effect on how closely patients adhere to the treatment regimen [1,4]. For example, reduction in frequency of dosing has been shown to correspond to increased adherence [5]. Treatment non-adherence has many negative consequences related to both clinical treatment outcomes and economic burden. It is well-established that non-adherence is associated with incomplete or inadequate treatment results [2–4,6–8]. Prolonged or repeated treatment leads to increased cost for care and was estimated to add up to $300 billion of avoidable economic burden to the healthcare system in the United States [8].

Several factors affect patients' ability and willingness to adhere to their treatment. Socioeconomic status and patient mindset have been shown to have a strong association with non-adherence. Financial hardship, lack of access to convenient transportation, and lack of social support are socioeconomic conditions that have been associated with non-adherence [2]. Behavioral factors such as perception of the treatment (and possible stigmas associated with it), perceived reduction in symptom intensity or extent, and medication side effects tend to influence patients to adhere less closely to treatment as instructed [2,6]. Some factors are also systematic to the health care experience and are therefore out of control of the patient. Lack of time between patients and physicians and poor care coordination, characteristics of a fragmented healthcare system, tend to negatively affect treatment adherence [2–4]. Patients often have limited time to

discuss treatment with their physician which can lead to inadequate understanding of treatment and increased likelihood of non-adherence. Discoordination and time constraints also impact physicians' ability to properly assess patient adherence to treatment which can lead to uncorrected regimens and behaviors. It should be noted that many of these factors are also associated with populations that are more vulnerable to infectious diseases.

In some cases, the medical condition for which the patient receives treatment can also inhibit the patient's ability to exactly adhere to the treatment. Treatment non-adherence has been shown to be disproportionately high among psychiatric patients due to impaired cognitive function [7]. Clinical consequences of non-adherence in patients suffering from psychiatric disease can be especially severe and may include relapse, hospitalization, suicide, or requirement of long-term care [7]. Dementia, which also impairs a patient's ability to manage their own condition and treatment, has also been associated with high rates of non-adherence [8]. For these diseases, treatment non-adherence can result in a negative feedback loop where the disease process negatively impacts the ability of the patient to effectively adhere to therapy which otherwise would improve or stabilize the cognitive decline associated with the disease. Non-adherence will tend to worsen these patients' symptoms which subsequently acts to further impair their ability to self-manage their condition. Patients with other diseases, such as tuberculosis (TB), may also be at increased risk for or afflicted with other debilitating diseases. TB has been strongly associated with HIV infection, both of which can act to physically weaken the patient. This is another example of a potential negative feedback loop which can form due to synergistic effects of being afflicted with multiple conditions. Furthermore, HIV infection has been shown to be a contributing factor to non-adherence to TB treatment [2]. Each of these examples shows that a patient's medical condition may act as a barrier to treating that condition. Based on this reasoning, interventions which focus on improving treatment adherence can both ensure that treatment is received properly and improve patient's ability to maintain proper adherence as they move through their treatment.

Given the many contributors to non-adherence, such as factors related to a patient's condition, socioeconomic status, or attitude towards treatment, a variety of interventions have been developed to address the issue of non-adherence. Because the high cost of treatment can often be a hindrance to treatment adherence, especially for certain socioeconomic groups which are disproportionately affected by financial hardship, organizations such as the World Health Organization (WHO) and its partners are making efforts to improve access to affordable healthcare

[1]. Other community-based organizations are often a resource for patients to improve education about treatment and address social needs [1]. Other interventions target healthcare providers as a source for improving treatment adherence. The WHO suggests that while education and training are available for healthcare providers to address adherence on an individual basis, these trainings are in need of refocusing. The trainings must more directly address how to collect data on patient adherence, how to interpret that data, and how to create tools for patients based on that data in order to create tailored interventions for non-adherence which are driven by the healthcare providers. Despite how widespread these interventions are, their implementation has shown to have only a weak effect on the problem of non-adherence. Each of these interventions tends to only address treatment adherence one-dimensionally; the factors which they address tend to be limited in scope despite the fact that adherence is a complex issue with many contributing factors. Furthermore, many interventions focus on education and self-management exclusively which has been shown to be a weak interventional approach [1]. There is therefore a need for organizational interventions which better address the complexity of the problem as well as the fact that patients' non-adherence may be the result of a diverse range of factors.

In addition to organization-based interventions, several technology interventions to address treatment non-adherence have already been attempted, each with varying levels of success. One such early attempt was the use of electronic adherence tracking devices. These devices are typically accessories which can attach directly to the medication dispenser (for example, an asthma inhaler) to record quantitative data about how and when patients take their medication. The main advantage to this technology was that a patient's adherence to treatment could be accurately assessed and be readily accessible to care providers. Early clinical studies had indicated that this technology may be effective for improving quality of care and intervening when treatment adherence is unsatisfactory. However, these devices introduced many concerns and additional burdens to both patients and care providers. Namely, these devices tend to be quite costly, add time to a consultation to set up the device and download data, and introduce a privacy concern among patients. Furthermore, long-term trials have not been performed to determine the devices' clinical effectiveness in practice [3].

Other technologies, whether already implemented or ideas for future innovation, may benefit from the advances introduced by adherence tracking devices. Electronic health information (*eHealth*) technology has potential for integrating electronic medical records with data collected

from tracking devices. Warnings and interventions can be automated and implemented without increased time burden to care providers. Such automated systems could also serve to provide reminders and treatment instructions to better improve adherence. Initial studies have even shown that automation may be a viable option for improving adherence [3]. The use of other sensors, such as biosensors or GPS, could provide data to predict when treatment is likely necessary and act as a prevention system. Such technology may be especially useful for conditions such as asthma that employ treatment as-needed. Nonetheless, each of these technologies suffer from practical limitations such as lack of resources to implement, privacy concerns, and additional burden to patient and care provider. There is also very little evidence to suggest that, if implemented and done so practically, these solutions would be effective in the long-term for improving treatment adherence.

From this discussion, it is evident that treatment non-adherence is a prevalent issue in the healthcare field which has detrimental effects for both patients and the healthcare system as a whole. Treatment adherence is also extremely difficult to enforce and has many contributing factors that would be difficult to address in practice. In some cases, the medical conditions for which treatment is being received can impair a patient's ability to adhere to the treatment, tending to worsen the condition. While several technologies have been developed or conceptualized which could address some of the major contributors to non-adherence, they have limitations and their long-term efficacy has not been well established. Therefore, there is a need for a technological intervention which is insensitive to treatment barriers, is well-controlled to ensure accurate adherence to treatment, and is minimally burdensome on patients and care providers.

Antibiotic Resistance

One major challenge in treating patients of infectious disease is the tendency for the bacteria that cause such diseases to be resistant (or develop resistance over time) to medications used in attempted treatments. Antibiotic resistant strains of bacteria emerge as the result of natural selection; as antibiotics are used to treat a bacterial strain, drug-sensitive bacteria will be eliminated while drug-resistant strains will continue to reproduce. Despite the fact that new antibiotics have been in development for decades, antibiotic resistance is ubiquitous in medicine; for every antibiotic developed to date, there is at least one recorded case of a resistant bacterial strain to that antibiotic [9]. In the case of widespread, global infections such as TB, antibiotic resistance is

especially detrimental to eradication attempts because implementation and distribution of universal, effective treatment in affected areas is difficult to achieve.

Antibiotic resistance develops as the result of a number of factors related to both individual patients as well as systematic issues related to healthcare providers. Antibiotic overuse is commonly cited as a cause of the emergence of resistant bacterial strains. Overuse accelerates the natural selection cycle for antibiotic resistant strains. While antibiotic prescription is regulated in the United States, antibiotics can be bought over the counter in other countries, opening up the opportunity for antibiotics to be more easily abused by allowing individuals to use them without consulting a doctor prior to use [9]. Inappropriate prescription of antibiotic treatment also contributes to antibiotic resistance. Studies have shown that in 30 to 50% of cases, treatment choice and duration indicated by healthcare providers are incorrect [9]. By incorrectly providing antibiotics to treat an infection, the patient may be at increased chance of developing antibiotic resistance due to exposure to sub-therapeutic levels of drug [9]. The problem of antibiotic resistance is further complicated by the fact that the rate of production of new antibiotics has declined in recent years [9]. Healthcare providers therefore have fewer alternatives to combat the increasing number antibiotic resistance bacterial infections that develop. Patients are also at a higher risk of developing antibiotic resistant strains if they were previously lost to follow up and/or require retreatment [10]. Despite being associated with a lower success rate and higher risk of developing resistance, attempts at retreatment are necessary from an eradication perspective to prevent further spread of antibiotic resistant strains of a disease to a patient's community.

Traditional treatment for bacterial infections often involves a single medication taken for prescribed amount of time. If further treatment is needed, physicians may prescribe a different medication to allow treatment to continue while avoiding the development of antibiotic resistant bacteria. However, the use of a single treatment over time accelerates selection of resistant bacteria. Any developed resistance has a tendency to prolong treatment and is associated with increased mortality rates [11]. One alternative to this traditional treatment is antibiotic cycling, a strategy in which prescribed medications are alternated at short periods. This approach has the advantage that the medications target a greater number of mutant bacteria with resistance to multiple drugs, improving the quality of treatment as well as decreasing the likelihood of developing resistance to any one medication [12]. Several studies have shown that antibiotic cycling may be viable for preventing the spread and development of antibiotic resistant strains of a disease [12]. Despite the

improved results to which this strategy may lead, drug cycling has the drawback of introducing additional complication to patients' treatment regimens. As discussed previously, more complex treatment regimens increase the risk of both intentional and unintentional treatment non-adherence. Furthermore, this increased risk would require more time devoted to patient monitoring and more coordination between providers and patients. Due to limited resources in many healthcare systems throughout the world, these additional demands on healthcare providers may be difficult to achieve.

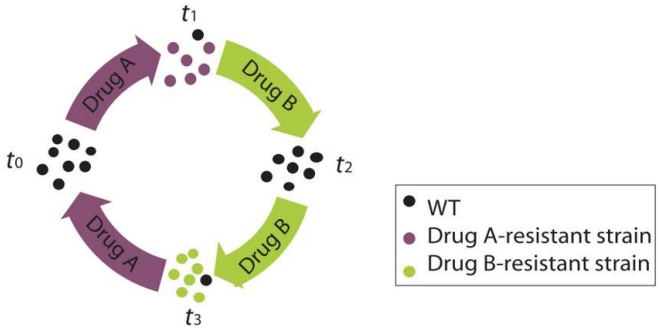

Figure 1-1: Model of drug cycling applied to strains of wild-type (WT) *E. Coli*. At t_0, WT strains are susceptible to drug A. Over time, strains develop resistance to drug A, but are sensitive to drug B. After switching to drug B, the same problem occurs. Cycling back to drug A incorporates a cycle where strains are always exposed to a drug to which they are sensitive. From Imamovic, L., and Sommer, M. O. A., 2013, "Use of Collateral Sensitivity Networks to Design Drug Cycling Protocols That Avoid Resistance Development," Sci. Transl. Med., **5**(204), p. 204ra132. [12]. Reprinted with permission from AAAS.

In current drug delivery schemes, patients commonly bear most of the responsibility in ensuring that treatment is accurately adhered to. This responsibility typically requires constant, active engagement in the treatment process and introduces the potential for human error. However, innovations in the drug delivery scheme can allow drug cycling to be a viable treatment strategy for patients by overcoming the barrier of human error. One class of devices which, by definition, reduces the need for human intervention is a gastric resident system. Such systems can be ingested or otherwise introduced into the gastrointestinal tract and are designed to safely reside there

without losing functionality or injuring the patient. In addition, gastric resident devices typically have precise control over the function they are designed to execute. One example of such a device was developed by Bellinger et al in the MIT Langer Laboratory [13]. Through a streamlined, "star-shaped" form factor, the device could successfully be introduced into the GI tract, reside there for approximately 10 days, and release malaria medication in a controlled method. This device will be discussed in more detail in Section 1.3. This example demonstrates how gastric resident devices eliminate the need for human input to administer medication. Such an automated, gastric resident drug delivery method that is reliable, consistent, and safe would also address many of the barriers associated with a drug cycling strategy. Such a system would have a positive effect on adherence to treatment regimens by shifting the burden of medication delivery from the patient to a well-controlled gastric resident device that is programmed with delivery instructions. By designing such a device for long-term treatment, patient intervention would occur with lower frequency. In this way, treatment non-adherence and lost to follow up incidents can be significantly reduced through technological intervention. In addition, the reduced risk of non-adherence may reduce the need for time demands of healthcare providers by removing non-adherence as a factor in follow up discussions. Therefore, the gastric resident device detailed in this thesis could provide flexibility in the drug delivery method chosen for a patient and allow drug cycling to be a viable option for treatment to overcome antibiotic resistance.

Prevalence of Tuberculosis in At-Risk Populations

One infectious disease whose eradication efforts are hindered by treatment non-adherence and antibiotic resistance is tuberculosis (TB). Significant resources are dedicated to global elimination efforts of TB, but the disease still remains a persistent public health threat. Recent estimates suggest that TB has surpassed HIV as the leading cause of infectious disease and is the ninth leading cause of death worldwide [14,15]. Despite the fact that incidence and mortality rates have been declining, global efforts have been unable to completely eliminate the disease. Because the disease continues to spread, over 8 million people each year become afflicted [2,15]. Additionally, patients with previously diagnosed cases of TB but who did not complete treatment are susceptible to and often experience reinfection [10].

Poor treatment adherence is one significant contributor to the persistence of TB. Several factors, some of which are unalterable and some of which could be the target of intervention, are

cited as predictors of poor treatment adherence. Homeless, impoverished, and unemployed people are one group that is prone to higher rates of non-adherence. One explanation is that outreach to these groups is typically more difficult due to reduced access to interventional resources. Unstable living conditions and a lack of a social support network may also contribute to poor adherence. Ethnicity, gender, and age have also been correlated to level of adherence [1,8]. For example, older patients tend to have lower rates of adherence than younger patients. Cultural belief systems may also influence how closely patients adhere to treatment [1]. This may be true of patients in developing countries who may prefer the use of traditional healing methods to modern medical intervention. However, many factors influencing adherence levels are alterable and could be the source of intervention to improve treatment adherence. Behavioral factors such as patient attitude towards medication and motivation to seek treatment have been correlated with medication adherence [1]. Patient education on treatment and ability to connect easily with clinicians and experts also have an effect on how well patients adhere to their treatment. Patients who are more educated on TB as well as the efficacy of medication tend to more correctly adhere to their treatment regimens [1]. Patients who can more readily communicate with clinicians and who are generally more satisfied with their health care provider are also more likely to adhere correctly to treatment. In addition to patient education, clinician education is a significant factor impacting adherence. Health care providers who lack skills and proper training necessary to counsel patients may be less likely to develop appropriate long-term treatment plans and enforce adherence [1]. Patient education and access to properly-trained, readily-accessible clinicians are especially likely to be insufficient for TB patients, a large proportion of whom reside in developing countries with less organized healthcare systems.

The persistence of TB is further attributed to the inability to combat multi-drug resistant TB (MDR-TB). In 2012, it was estimated that MDR-TB accounts for approximately 3% of all new TB cases and 20% of existing cases [15]. These cases are particularly difficult to combat because strains of MDR-TB are typically resistant to isoniazid and rifampicin, two drugs which are typically the first-line defense against new TB cases. Identification of MDR-TB cases has shown to be the first difficulty in treating drug-resistant TB. In 2012, the number of reported MDR-TB cases accounts for less than 30% of the estimated total cases [15]. This statistic indicates that methods for diagnosing drug-resistant TB may be ineffective. Because MDR-TB may be less likely to be diagnosed correctly and is typically untreatable by first-line drugs available in standard TB

treatments, drug-resistant TB poses a significant concern with respect to controlling and eradicating TB worldwide.

Given the severity of the disease as well as the difficulty of eradicating it on a global scale, several interventions have been developed worldwide to address the persistence of TB. One such strategy is Directly Observed Treatment, Short-Course (DOTS) intervention. Recommended by WHO, this strategy details diagnostic methods, standardized, supervised treatment, and patient monitoring methods for global eradication efforts. It was reported that because nearly 180 countries have adopted DOTS intervention, over 17 million patients were started on effective treatment during the 8 years following its implementation [15]. Similar global treatment programs have since been developed, drawing inspiration from DOTS and expanding on its founding principles to address the link between TB and HIV, MDR-TB, and the needs of vulnerable populations such impoverished, homeless, and/or elderly people [14,15]. Despite these advances in global outreach, the decline in the tuberculosis incidence and mortality rates have been low. This fact suggests that these global interventions are incomplete. One reason is that drug-resistant TB is not easily addressed through a standardized treatment regimen. It is still an open question of how to address this issue on a global scale, and it may be that by incorporating drug cycling into the standard treatment regimen could partially address this concern. Another reason could be that despite global commitment to eradication efforts, funding continues to be limited especially for efforts in developing countries. Limited funding can impact resources and education for healthcare providers as well as effectiveness of outreach efforts.

Because of the severity of its persistence as well as the factors which hinder progress towards its eradication, TB serves as a highly relevant case study for which this design project could be applied. In addition, TB is an example of a disease requiring large doses of drug for treatment. TB in many cases will require 100 grams per month of drug to be administered [16]. The TB eradication effort could benefit greatly from a low-cost, non-invasive technological approach to delivering medication in a controlled, repeatable way. The device designed in this project attempts to address the need to overcome medication non-adherence and antibiotic resistance as it relates to eradicating epidemics of infectious diseases such as TB. With the device being a gastric resident medication delivery system, it significantly reduces the need for patient or physician input to ensure medication is delivered correctly. In the same way, the device can also address the high TB incidence and mortality rates among vulnerable groups by offering a low-cost,

long-term medication delivery solution that reduces the likelihood of patients becoming lost to follow up.

1.2 Design Requirements

Gastric residence devices interact with the body through four key modules related to their functionality:

- Administration through the esophagus
- Residence in the stomach
- Drug delivery/release in the stomach
- Removal (Retrieval through the esophagus vs. dissolution of macro-structure into excretable segments)

Each stage introduces different design requirements which the device must adhere to in order to be functional and interact safely with the patient. Each module and the corresponding design requirements are discussed in the following sections.

Design for Administration

Any device designed to be delivered to and reside in the stomach is subject to the environment imposed by the esophagus. One important design constraint relates to the size of the esophagus. The typical lower limit for the diameter of the esophagus is approximately 20mm [13,17]. At least one critical dimension of the device must be less than this value in order to safely pass through the esophagus to the stomach. In addition, the device housing must be linearized to align with the fact that the esophagus is a long, approximately straight tube with known diameter. During the process of passing through the esophagus, the device may also experience external pressure due to peristalsis in the esophagus. Estimates suggest a reasonable pressure to use for the design of the device's outer housing is approximately 15 kPa [17].

Design for Residence

Because the device interacts with the environment of the stomach, careful consideration must be made to ensure compatibility of the device with the environment as well as safety during residence in the GI tract. The mechanism for retention must be designed such that the device does

not block food or liquid passage during residence time. Only chemical resistant materials or coatings such as PTFE should be used for components of the device which are exposed to gastric acid to prevent harm to the patient and damage to the interior of the device. To protect the lining of the stomach from damage, all external surfaces of the device must have smooth geometry.

While the device is in residence, it experiences forces due to peristalsis which attempt to move the device through the pylorus into the intestines. The design of the star device by Bellinger was designed to conservatively withstand a peristaltic force of 1.5N [13]. In order to provide a factor of safety and account for this device's large size, the device was designed to withstand a 3N peristaltic force.

Design for Pulsatile Drug Delivery

The goal of this gastric residence device is to dispense a loaded pill once per day for at least 5 days. For in vivo testing, the drug chosen to be loaded into the pills was doxycycline hyclate due to its well-known clinical use of treating bacterial infections [18]. The target pill for proof of concept has a cylindrical shape and is approximately 4mm in diameter and 6mm in length, with a total mass of approximately 100mg and 90% concentration of drug. This specific formulation was chosen to allow the released pills to elicit a high enough response in blood serum levels during in vivo tests as well as align with clinical dosage levels. All pills must be able to fit within the housing of the device.

Backflow prevention is an important consideration in designing this gastric resident device because solid medication is being delivered rather than liquid medication. The device needs to be able to expel solid medication in a controlled manner while also preventing gastric acid from flowing into the device. This constraint serves as a safety requirement both for the device and the patient. Backflow of acid into the device may cause premature, uncontrolled dissolution of loaded medication which has not be dispensed. This situation may lead to inadvertent overdosing or compromised control of medication dispensing. Backflow into the device may also compromise more sensitive components such as electronics, as some components are not intended to make contact with the environment of the stomach.

From an electronics perspective onboard power supplies must be extremely compact while still supplying the necessary power for any electronics, microcontrollers, and electromechanical components. For patient safety, actuators should be compact enough to function and reside within

the device. Furthermore, if electronics are used within the device, all currents supplied from the power supply must be below minimally accepted values for biosafety.

Design for Retrieval

In vivo tests of this device were conducted in a terminal animal experiment. Therefore, it was not necessary for the scope of this project to design the device to be retrieved. A number of strategies have been implemented in similar devices that could potentially be leveraged in the later optimization of this device. One strategy is endoscopic retrieval. A device previously designed in the Langer and Traverso Laboratories makes use of a magnetic attachment, allowing a magnetic to attach to the gastric resident device and retrieve it through an endoscope [19]. Another strategy is to allow the device to break down and/or pass through the pylorus at the end of residence. Another device designed in the Langer and Traverso Laboratories uses this principle to design arms made of temperature sensitive biomaterials which dissolve after a certain amount of time and allow the corresponding device to pass through the pylorus [20].

1.3 Overview of Prior Art

Ultra-Long Lasting Gastrointestinal Drug Delivery for Malaria Treatment

One approach taken to implement long-lasting, in-vivo drug delivery through a gastric resident device was developed by Bellinger et al in the Langer and Traverso Laboratories at MIT [13]. The device served as a capsule to house individual dosages of ivermectin, a medication for preventing malaria infection and transmission. The capsule makes use of tunable linkers which connect polymeric dosages to an elastomeric base. As the linkers are exposed to different pH levels, they will dissolve in controlled manner to release the dosages into the GI tract for administration. When administered, the capsule opens up into a star-shaped configuration which prevents the device from passing into the small intestine until the dosages are separated. Because all of the components in the capsule are strictly limited to a 2cm maximum critical dimension, all components are able to pass safely through the GI tract for absorption by and evacuation from the body. Results of in-vivo studies showed that this capsule was capable of delivering 10 to 14 days of medication to maintain necessary levels of blood serum concentrations.

This approach to gastric resident drug delivery has many advantages. The capsule first demonstrates an important safety mechanism in which the dosages only pass to the small intestine

when intended. Because the star-shaped configuration holds the expanded capsule in the stomach until dissolution of the linkers allows capsules to be absorbed by the GI tract, the device successfully prevents inadvertent over-dosage in the event of a failure. The device further demonstrates that gastric residence can be achieved in a way that is non-invasive to the patient during in-vivo use. The capsule is sized to allow it to be ingested, and it will pass through the GI tract without further intervention. The main advantage to this gastric resident device is that medication adherence is virtually guaranteed because the release of the drug into the GI tract is controlled by the components in the capsule instead of relying on human adherence to dosage instructions. Despite these advantages, the device is limited in its flexibility. The main limitation is the fact that the dosage levels it can hold are small compared to the goals for this project. In addition, its ability to be scaled to longer gastric residence times is limited by the tenability of the material used for the linkers. Drug is loaded into the capsule in a way that is suitable for the ivermectin dosages used in this particular study. Thus, its ability to accommodate medication with other form factors may be limited. Nonetheless, the device designed by Bellinger et al serves as a notable example of a gastric resident device and can help guide the design of features in this project which allow a device to safely reside in the stomach and GI tract.

Wireless, Endoscopic Systems with Drug Delivery Capabilities

One type of medical device which has recently begun to include mechanisms for drug delivery is the wireless endoscope. While their primary purpose is to detect and diagnose gastrointestinal complications, these systems may benefit from being able to deliver interventional medication after diagnoses. In many ways endoscopic capsules are well-suited for the introduction of drug delivery capabilities. Their size and form factor have already been optimized for minimally invasive oral ingestion. These wireless endoscopes also contain many onboard sensors, electronics, and transmitters to perform their diagnostic processes. They therefore already include the basic framework for housing electronics in a harsh, acidic environment like the gastrointestinal tract. However, one major challenge is to incorporate this drug delivery mechanism in a way that does not significantly increase the size of the devices or interfere with existing components involved in the imaging process.

One wireless endoscope system has been developed by Woods et al which successfully incorporates two additional mechanisms to deliver liquid medication through a needle [21]. A

figure from the paper detailing this device is shown in Figure 1-1. One mechanism is a needle positioning mechanism, which makes use of a custom cam feature to actuate and retract a needle and provide the necessary force to penetrate the wall of the gastrointestinal tract. The other feature is a holding mechanism which allows the endoscope to be stabilized and oppose peristaltic pressure while in the gastrointestinal tract. This mechanism uses a linkage of arms driven by a geared micromotor which expands the arms to increase the effective size of the device. Each mechanism is driven by a separate micromotors which are very compact and are oriented to optimize space in the device. The endoscope is also able to maintain its diagnostic equipment by housing the imaging and processing components in the domed end of the device. The system housing is approximately 32mm in length and 11mm in diameter, indicating that the design retains a highly compact form factor compared to traditional endoscopic capsules.

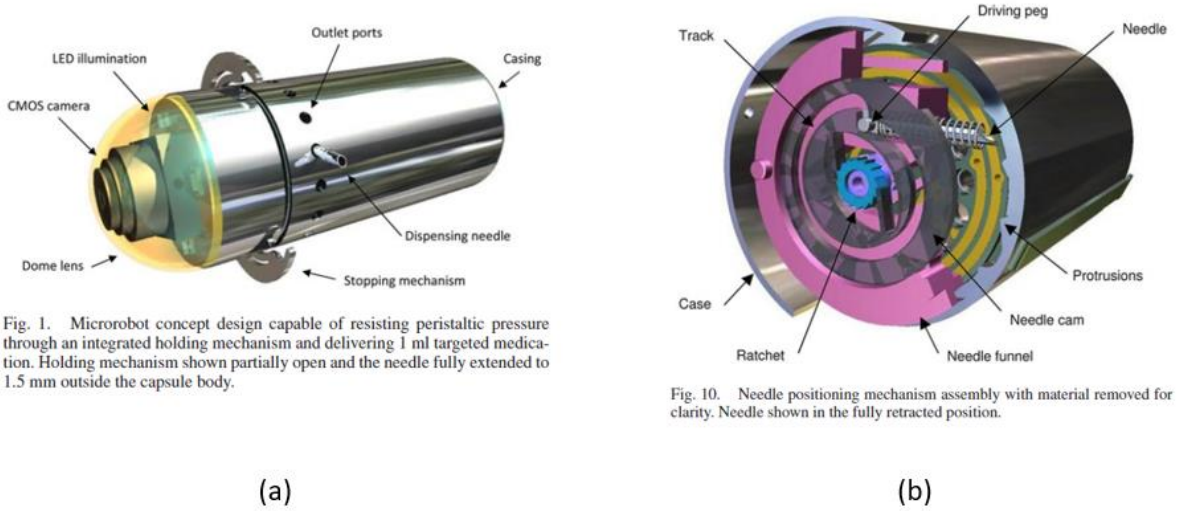

Figure 1-2: Schematic of the wireless capsule endoscope system developed by Woods et al. (a) A general layout of the device, including locations of imaging technology and drug delivery mechanisms. (b) Schematic of the needle position mechanism used for drug delivery. Figures reproduced with permission from [21], © 2012 IEEE.

Other work developed by Munoz et al demonstrated another strategy for controlling the drug delivery within a compact, ingestible device [22]. The device detailed in this work made use of a permanent magnetic connected directly to a mechanism similar to a piston cylinder mechanism. The permanent magnet functions similar to a motor to actuate the motion of the sliding components when exposed to a precisely controlled, external magnetic field. It should be noted that the novelty of this device is not only in the fact that drug release can be accurately controlled, but that the release can be actuated from an outside the patient's body. This device was specifically developed to deliver approximately liquid medication with a drug reservoir that can be customized based on mechanical components within the device. The capsule developed in the work by Munoz et al ultimately did not have diagnostic capabilities as in a traditional endoscope, but the mechanism was designed with the intention of including it in a device such as an endoscopic capsule that houses additional modules such as imaging sensors.

Each of these endoscopic systems takes a novel approach to including a compact drug delivery mechanism, and each device has its advantages from which insight can be gained. One commonality between the designs is that the actuation of the drug releasing mechanism is carried out by a rotary element in a capsule shaped housing. One reason for this may be that rotary actuators tend to be more space efficient in cylindrical spaces compared to other options such as linear actuators. Additionally, customization of torque or force output can be achieved more compactly with cylindrical geometry. The mechanisms used in each of these devices, such as the cam and sliding crank, also assume highly nonlinear force output over a single rotation despite the fact that mechanisms exist for converting torque into a constant force output with linear motion. The tradeoff to this design choice is that the reciprocating, linear motion can be achieved with unidirectional rotary motion, simplifying motor control. It may also be that the nonlinear force profile allows actuator torque output to be utilized most efficiently by providing higher force output only where it is needed. Finally, the device from Woods et al introduces a method for stabilizing the device within the stomach. Such a mechanism can also be used to prevent the device from passing through the GI tract without hindering gastrointestinal flow.

One key limitation to these devices, however, is the fact that medication can only be delivered in liquid form. While these mechanisms could be adapted to handle the dispensing of solid medication, they would require many additional features to make such adaption successful. Because these capsules dispense drug in liquid form, concern over backflow of gastric acid is less

of a concern; liquids can typically be expelled at a high enough pressure that backflow will not occur. Despite these noteworthy differences between the design requirements of these devices and this project, these examples of existing drug delivery systems in ingestible devices illuminate important trends in the design of compact devices. Such trends can help guide the design of a mechanism which allows medication to be released safely and in a controlled manner regardless of the form it takes.

Controlled Drug Delivery Capsule for Powdered Medication

The differences between delivering liquid and solid medications can be resolved by observing technologies which control the delivery of powdered drug. Powdered medication is subject to many of the challenges of dispensing solid medication, such as backflow prevention and requiring a pushing force to motivate the exit of the drug, while still being reminiscent of a continuous medium such as a liquid. One device invented by Dijksman et al demonstrates a mechanism aimed at powder medication delivery [23]. The device consists of one or more chambers separated by thin foil where each chamber contains a dosage of drug. To release the drug, the foil is punctured with a joule heating process by passing a large current through an adjacent heating wire for a very short duration. The powdered medication within the chamber is then exposed to the environment of the stomach and washed out of the chamber. The electronics are housed in a module in the device which is isolated from the gastrointestinal environment.

This system has many noteworthy advantages. As is common for many ingestible devices, the device has a cylindrical, capsule-like form factor which is ideal for delivering the device. Because the mechanism for medication delivery is mostly performed by electronics, the device is highly compact and most of the volume is dedicated to storing the medication. However, safety of the device in the event of a malfunction is an important concern. Because the device is designed to deliver high currents, although for a short amount of time, the potential for harm to the patient in the event of a malfunction cannot be ignored. In addition, because the device relies on joule heating and high currents, it is likely that it requires a significant amount of energy compared to mechanical means of actuating drug delivery. Nonetheless, this device provides insight into the efficient organization of solid medication into a device and offers one way in which the issue of backflow prevention can be addressed.

1.4 Statement of Project Scope

The goal of the project detailed in this thesis was to develop a prototype of a pulsatile, controlled drug release device which meets design requirements given in section 1.2 and functions at bench-level. After functionality at bench level was confirmed and proof-of-concept was achieved, we chose to extend the project to demonstrate proof-of-concept in vivo. Many concepts detailed in this thesis, such as those associated with onboard electronics integration and device retention, were not implemented by the time of completion of this thesis. However, some preliminary design work was done with each of these concepts, and future work immediately following the submission of this thesis focused on implementing these concepts for realization of a self-contained, autonomous prototype for in vivo testing.

2. Design of Pulsatile Pill Release Mechanism

2.1 Rotating Disk Concept

Overview of Concept

The first concept devised for a mechanism to release pills is shown in Figure 2-1 and is termed the "rotating disk" concept. The mechanism consists of three disks. Two disks or surfaces (shown in red) are stationary and contain pill-shaped cavities whose centers are offset from each other by 180 degrees relative to the central axis of the disks. The third disk (shown in blue) rotates about its center and contains one pill-shaped cavity. As the third disk rotates, its cavity will align with one of the two stationary disks to allow a pill to pass through the mechanism.

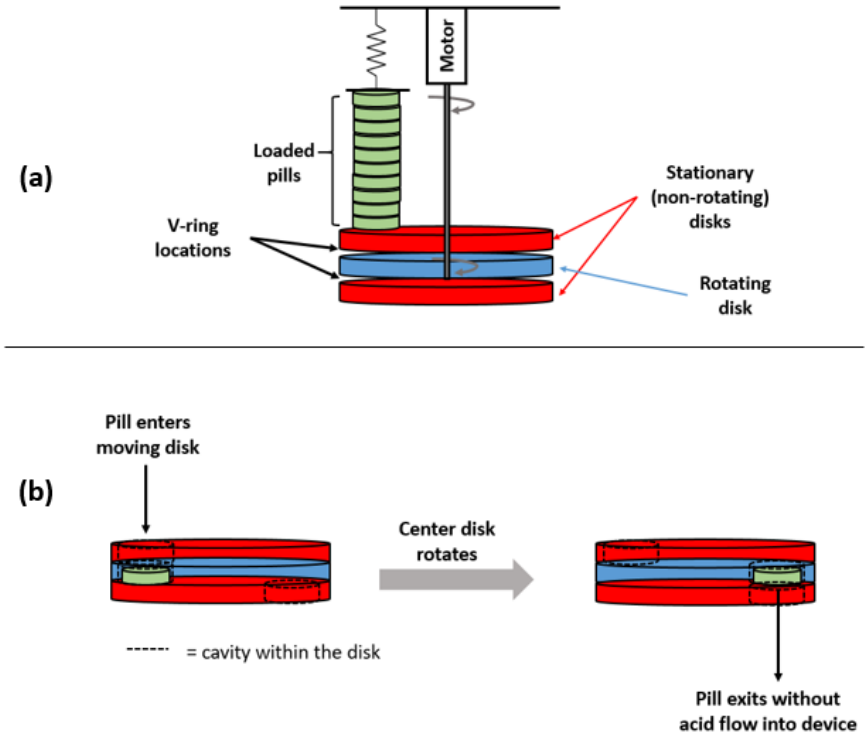

Figure 2-1: (a) Schematic of the components of the "rotating disk" concept and how they interact. (b) A schematic of how the three disks are used to load and dispense a pill from the device.

This concept was considered first because it is based on cylindrical symmetry. With this type of symmetry, motors can be used to drive the mechanism while achieving the desired long and thin form factor. Additionally, because motors are one of the most common types of actuators,

an appropriate motor that is compact and cost-effective can easily be incorporated into the mechanism. The offset placement of the cavities in the three disks was chosen in order to prevent backflow of gastric acid. This concept ensures that the pill loaded in the rotating disk cannot be open to the device's interior and the environment of the stomach simultaneously.

Torque Analysis of Concept

The rotating disk concept relies on a motor supplying torque which can overcome the frictional torques contributed by all sources friction. That is:

$$\tau_{motor} = \sum_i R_i F_{f,i} + \sum_j \tau_{f,j} \tag{2-1}$$

where τ_{motor} denotes the torque supplied by the motor, $F_{f,i}$ denotes a frictional force acting on the rotating disk at an effective distance R_i from the center of the disk, and $\tau_{f,j}$ denotes a frictional torque acting on the disk. In implementing this prototype, we would not expect any sources of frictional torques because most friction will be the result of friction forces at contact points between surfaces. Assuming $\sum \tau_{f,j} = 0$ and that the frictional force can modeled as being proportional to the reaction force normal to the surface, the above equation simplifies to:

$$\tau_{motor} = \sum_i \mu_i R_i F_{R,i} \tag{2-2}$$

where μ_i is the coefficient of friction between the two surfaces in contact and $F_{R,i}$ is the reaction (normal) force between the two surfaces. In general, the reaction forces depend on the geometry of the surfaces in contact.

In one chosen configuration, four O-rings were placed as shown in Figure 2-2, such that the surround the pill but are fixture by the stationary disks. As the center disk rotates, the O-rings slide against it while some reaction force acts between the surface. While the O-rings may contact the disk surface at many points, we simplify analysis by assuming we can model the interaction as occurring at a single, effective point at some distance R_{OR} from the disk center. From the torque relationship given above, the motor torque can be estimated as:

$$\tau_{motor} = 4\mu_{OR}R_{OR}F_{OR} \quad (2\text{-}3)$$

where μ_{OR} is the coefficient of friction between the O-ring and the disk material and F_{OR} is the reaction force on a single O-ring.

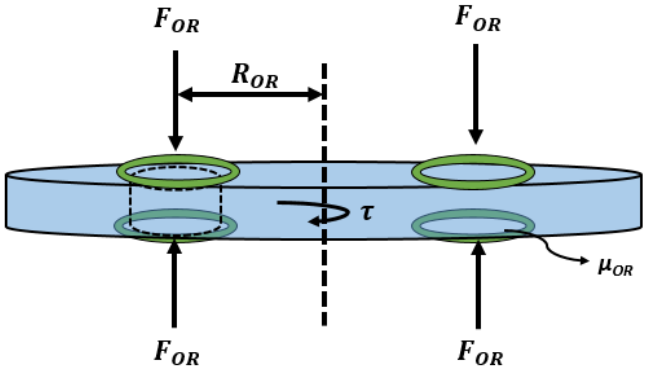

Figure 2-2: Free body diagram of O-ring placement and interaction in rotating disk concept.

A number of observations can be made from this relationship. First, motor torque is constant while in operation. Second, the above variables are either not controllable or do not introduce a degree of freedom for design. The coefficient of friction and effective radius are functions of material choice, device geometry, and pill geometry. The reaction force is, in theory, a free variable, but is directly proportional to the desired level of safety against backflow. As greater safety against backflow is desired, F_{OR} must increase (usually nonlinearly). Therefore, there is a tradeoff between backflow prevention and motor power.

Evaluation of Concept

This first attempt at a pill release mechanism (shown in Figure 2-3) had many advantages while also revealing many design considerations that required further work. The rotating disk concept was advantageous in that it systematically separated the device's interior from the stomach environment. In addition, control of motion of the mechanism could be implemented simply because disk rotation was unidirectional. The strategy also follows the desired form factor in that

the disk size is only dependent on the size of the drug being delivered and the method of administration, while the length of the device is scalable depending on the amount of drug to be loaded. The length of the device does not impact the pill release mechanism's functionality.

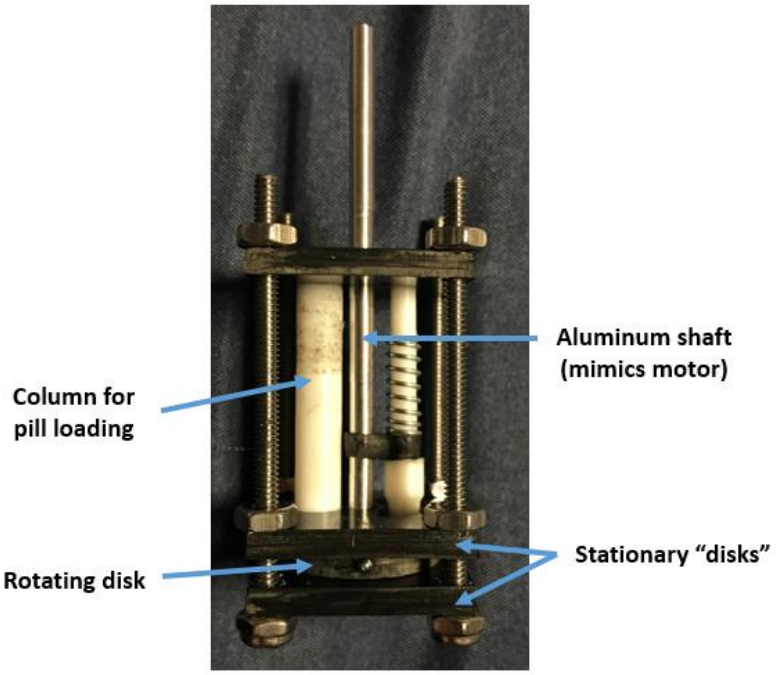

Figure 2-3: Functional prototype of rotating disk concept. The mechanism is shown on the bottom part of the device. An aluminum shaft functioned as the "motor" for bench level testing. A separate, spring-loaded shaft (shown on the right) was added to help force pills from the device.

One important limitation of the mechanism was its inability to force pills from the device once they are rotated into the hole in the bottom stationary disk. Furthermore, passage of the pill into this hole is dependent on gravity, which cannot generally be guaranteed while resident in the stomach. During testing, pills would also become trapped in the exit hole by sticking to the walls. One tested solution is shown in Figure 2-3 and consisted of a spring loaded shaft which extends into the pill hole during pill ejection. However, this solution is not viable for an autonomous system as it would require a separate actuator. Another, proposed solution was to include a spring-loaded flap on the underside of the rotating disk that extends into the exit hole during pill exit. However, one major concern of this strategy is that the flap would be introduce a high contact force with a

moving surface, leading to increased friction within the mechanism. This pill release strategy nonetheless reveals the need for a feature that forces pills to exit, even at the tradeoff of less backflow management.

Another limitation of this strategy is that motor power in this mechanism goes to overcoming friction instead of contributing to a productive motion. Therefore, as mechanism inefficiencies increase, the power required by the motor also increases. These inefficiencies can also be difficult to predict and model entirely, so safety factors would need to be large to compensate. Finally, for this release mechanism to be effective at backflow prevention, seals must be used against the rotating disk. Therefore, backflow prevention seals introduce friction which is dependent on the desired protection against leakage. All of these factors lead to a mechanism which is ultimately inefficient and would require high power motors that are not practical for implementation.

2.2 Pushrod with Linkage Concept

Overview of Concept

The rotating disk concept revealed a need for the pill release mechanism to actively force the pills out of the device. At the same time, a mechanism driven by a long and thin actuator (such as a motor) has been shown to most effectively utilize the limited space in the device while achieving the desired form factor. A new concept was therefore devised which loads a pill into a channel and reciprocates a pushrod to force the pill out of the device. Because the pushrod motion occurs in a different direction than the long axis of the device, a linkage is necessary to transmit actuator motion to the pushrod.

Linkages generally transmit actuator dynamics in a nonlinear fashion, so careful consideration must be given to the type of actuator the type of linkage. Two different types of linkages were initially considered which reduce the required number of links and transmit actuator motion to a "pushing" motion at the output. One option, shown in Figure 2-4, involves two linkages connected to a linear actuator. As the linear actuator extends or retracts in one direction, the output link can also reciprocate, but in the desired direction. The second option, shown in Figure 2-5 and discussed in more detail in the next subsection, is a traditional four-bar linkage and involves three links connected to a rotary actuator (such as a motor).

The second option was ultimately chosen as the linkage to be implemented for the pushrod concept for many reasons. First, motors (and other rotary actuators) generally are manufactured with much more variety and can be made much more compact than linear actuators. Second, the dynamics of the linear actuator linkage are not as conducive to the small space available for the mechanism. An analysis of the forces and kinematics involved in such a system reveals that force output is inversely related to the motion of the output link. That is, if the linkage operates where high force is exerted at the output link, the displacement of the link is much lower than if the linkage operates where the output force is lower. This situation would require that either the mechanism itself takes up a large amount of space or the forces involved must be low. Third, the actuator requires more complex control because it needs to have reversible current to achieve both extension and retraction. In comparison, the rotary actuation linkage operates uni-directionally; rotation of the motor in a single direction can achieve both a pushing and a retracting motion at the output linkage.

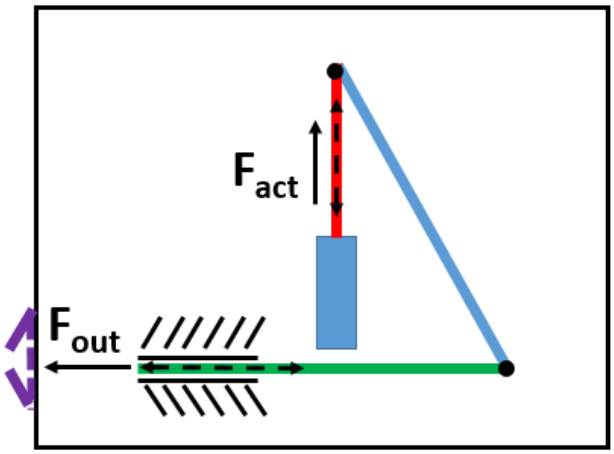

Figure 2-4: Schematic of linkage concept involving a linear actuator.

Force Analysis of Linkage with Rotary Input

Motor torque is converted to linear force for pushing pills out of the device through the four-bar linkage mechanism. In general, this force will depend on the geometry and configuration of the linkages. To analyze the power transmission, the linkages were approximated as two-dimensional rigid bodies with frictionless pin joint connections. The assumption that the pin joints

are frictionless is validated in Appendix A. In addition, the interaction between the push link (shown in green in Figure 2-5) and the rigid slider constraint is considered frictionless for now but will be relaxed in future analysis. The motion is also assumed to be quasi-static, which is justified by assuming the links are of such small mass that inertial effects are negligible. Figure 2-5 shows a schematic of this analysis along with free-body diagrams of each link.

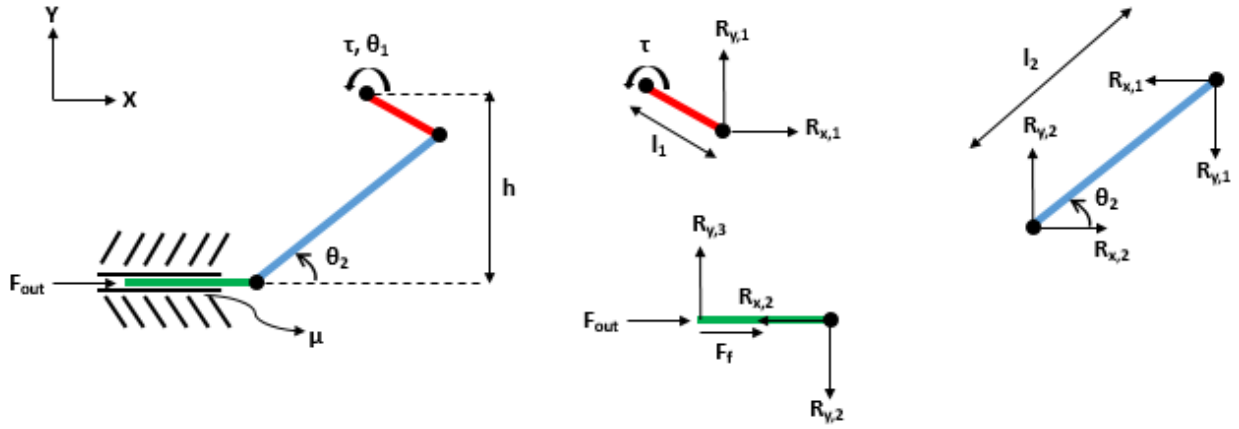

Figure 2-5: Schematic of simplified four-bar linkage for analysis. The red, blue, and green links are numbered 1, 2, and 3 (respectively) for analysis.

By summing forces on the linkages as well as summing moments about the point where link 1 attaches to the torque source, the following relationships are found:

$$\tau + l_1 \cos\theta_1 R_{y,1} - l_1 \sin\theta_1 R_{x,1} = 0 \tag{2-4}$$

$$R_{y,1} = R_{y,2} = R_{y,3} = -\frac{\tau \tan(\pi - \theta_2)}{l_1(\cos\theta_1 \tan(\pi - \theta_2) + \sin\theta_1)} \tag{2-5}$$

$$R_{x,1} = R_{x,2} = R_{x,3} = \frac{\tau}{l_1(\cos\theta_1 \tan(\pi - \theta_2) + \sin\theta_1)} \tag{2-6}$$

$$F_{out} = R_{x,3} \tag{2-7}$$

Furthermore, the geometric constraints between links 1 and 2 imply:

$$h + l_1 \sin\theta_1 = l_2 \sin\theta_2 \tag{2-8}$$

$$l_2 \geq h + l_1 \tag{2-9}$$

Solving the above equations gives a relationship between force output and torque input:

$$\frac{\tau}{F_{out}} = l_1 \left[\sin\theta_1 + \cos\theta_1 \left(\frac{h + l_1 \sin\theta_1}{\sqrt{l_2^2 - (h + l_1)^2}} \right) \right] \tag{2-10}$$

A few notable conclusions can be drawn from this result. First, the relationship between the output force of the pushrod and the input torque of the torque source is linear. As higher output forces are needed for the mechanism, the torque requirement for the motor scales proportionally. Second, the relationship between these two quantities is also configuration dependent. As the motor rotates and the links change orientation, torque required to achieve a certain force output may change even if the force requirement remains constant. Third, the configuration dependent scaling factor (i.e. the right side of equation 2-10) is nonlinear and is equal to zero at a number of points along a single rotation of the motor. This fact indicates that the four-bar linkage has an added advantage in power transmission in that it can achieve higher force output for a given torque input by using the stiffness of the links to compensate for certain force components. In other words, the stiffness of the links can be used such that the motor does not need to provide power for overcoming all reaction forces in the linkage.

Friction Analysis of Sliding Component

To examine non-ideal effects on the four-bar linkage from sources of friction, previous assumptions need to be relaxed. A significant source of friction in the mechanism could be from sliding friction between the push rod and the walls to guide the linear motion of the push rod. This effect can be modeled as a frictional force acting on the push rod in a direction that is always opposite the horizontal force acting on the rod. Equation 2-7 can be modified such that:

$$F_f = sign(R_{x,3})\,\mu_s\,|R_{y,3}| \tag{2-11}$$

$$F_{out} = R_{x,3} - F_f \tag{2-12}$$

where F_f is the frictional force acting on the push link. Using equations 2-4 through 2-6 (which do not change from the ideal case), this system can be solved to give a relationship between output force and input torque for this non-ideal case of the system. This system was simulated in MATLAB and compared to the ideal case as shown in Figure 2-6.

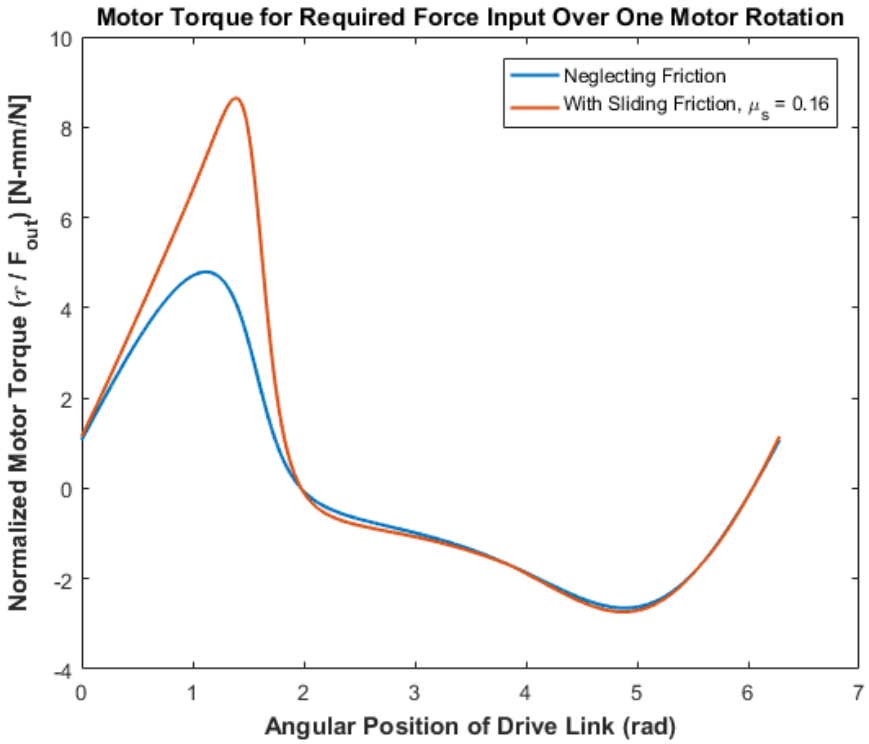

Figure 2-6: Simulation of the four-bar linkage analysis for the ideal (frictionless) case and non-ideal (with sliding friction) case. The simulation used l_1 = 2.6 mm, l_2 = 4.45 mm, and h = 1.7 mm from the actual values used in the design of the device. μ_s = 0.16 was used as a conservative estimate of friction in the sliding components (see Appendix B).

Analysis of Jamming Prevention Strategy

Pills loaded into this device are stacked such that their cylindrical faces are in contact. This orientation is advantageous for many reasons. First, because the pill size is 4mm by 6mm, the column containing the pills can hold 50% more pills compared to the orientation in which the flat faces of the pills are in contact. Second, any frictional resistance experienced when the pills contact and slide against a flat surface will be reduced because the pills can roll (rather than slide) and the area in contact with the flat surface is much smaller than in the alternative orientation. However, in this orientation the pill release mechanism functions by pushing the pills in a direction perpendicular to the direction in which they are loaded. There is therefore potential for the device to mechanically jam if precautions are not taken.

While the length of the push link does not affect the performance of the mechanics of the force output, its geometry is crucial for the prevention of jamming. In particular, because the link interacts directly with the pills it needs to be somewhat sensitive to pills with diameters smaller than its height as well as variations in pill size. When a pill with a diameter smaller than the channel height is fully loaded into the channel, a second pill is also partially loaded into the channel due to the spring loading. When the push link with a rectangular end attempts to release the pill, it is geometrically blocked by the partially loaded pill. To overcome this problem, the end of the push link was designed to have a slight chamfer. The chamfered surface acts like an inclined plane up which the partially loaded pill can roll up as the bottom pill is pushed out of the device. Figure 2-7 illustrates this problem and the designed solution.

One consideration with this solution is that part of the output force of the push link must be able to overcome the spring force in the pill loading column. Force analysis on the partially loaded pill while in contact with the chamfered surface can provide insight into how to choose the angle of the chamfer and optimize a spring force for pill loading. Consider Figure 2-8 which shows a free-body diagram of the partially loaded pill. The effects of the spring and push link force are modeled along with two sources of friction. One force is a static friction force (F_f) between the wall of the pill column and the pill, which can become significant because it induces a torque which opposes the rolling motion of the pill. The other source is rolling resistance between the pill and the push link. For the pill to experience rolling motion, the sum of moments about the center of the pill must be less than zero in the defined reference frame. This constraint provides the following design criterion:

$$\frac{F_{spring}}{F_{out}}[\mu_s(\sin\theta + \mu_R\cos\theta) - \mu_R] + [\mu_s(\cos\theta - \mu_R\sin\theta) + (\mu_R + \mu_s)\tan\theta - 1] < 0 \quad (2\text{-}13)$$

where μ_s is the coefficient of static friction between the pill and the wall of the pill column, μ_R is the coefficient of friction between the pill and the push link, θ is the angle of incline of the push link, F_{spring} is the maximum spring force exerted on the pill, and F_{out} is the component of output force from the push link used to push a pill against the spring force to overcome jamming. Note that F_{out} may be lower than the total output force achieved by the pill release mechanism because the push link may simultaneously be pushing a pill against the spring force while also pushing a pill against a sealing mechanism near the exit (such as a spring loaded door).

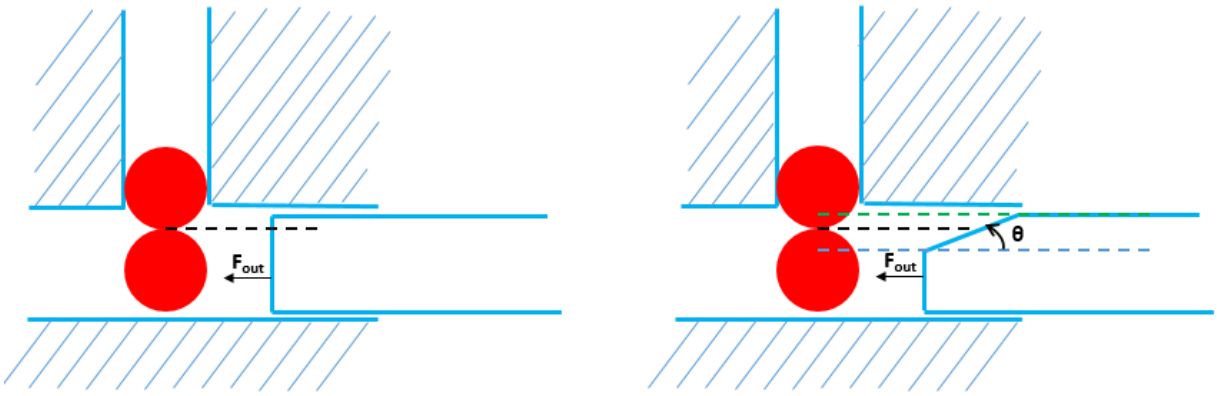

Figure 2-7: Schematic of jamming prevention strategy. The left side shows the case where there is no chamfer on the pushrod and why there is potential for jamming. The right side shows how the chamfer can overcome jamming by allowing pills to roll up an "inclined plane".

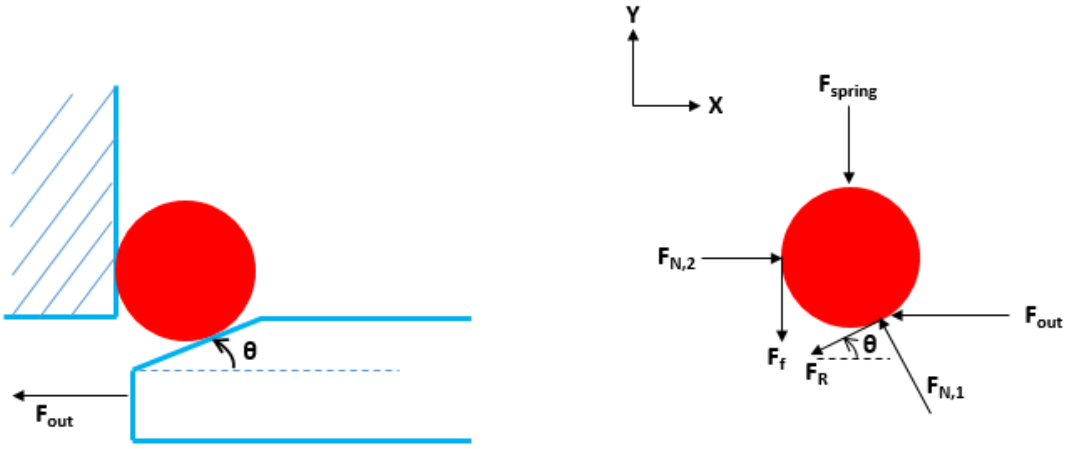

Figure 2-8: A free body diagram of the model used to analyze the jamming prevention strategy.

Estimation of Maximum Output Force

The force experienced at the push link (F_{out}) can be the result of two separate events: ejecting a pill from the device and pushing a pill against the spring loaded pill column. Due to the sequential nature of the device's pill loading design, the force required from the drive link for each of these events can be considered reasonably independent. That is, while the device is pushing a pill against the spring loaded pill column, it is not yet at a point where it will be pushed against the exit doors to be released from the device. While a pill is being ejected from the device, the pill column is stationary and has little impact on the output force.

As pills are released, they are pushed against two doors. Multiple door configurations were considered throughout iteration on the device. A simple model can be developed to estimate the maximum output force needed to overcome the deformation of the doors. Geometrically, a pill will be forced out of the device when the line connecting the ends of each door pass the center of the pills diameter. At this point (shown in Figure 2-9), the compression against the body of the pill becomes unstable and it is forcefully expelled from the device. The maximum torque due to spring loading is also achieved at this point.

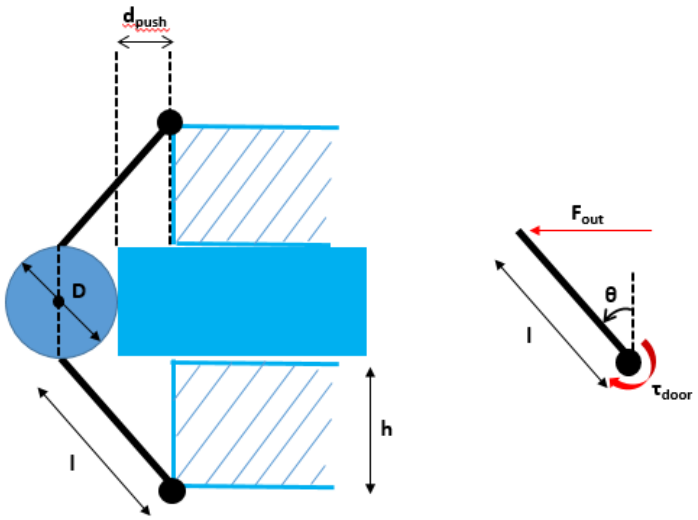

Figure 2-9: Schematic of the exit door model. l denotes the length of the pivoting portion of the exit door, and h denotes the distance of the pivot point to the base of the pill hole. d_{push} denotes the distance which the pill pushes past the exit hole to help force the pill out of the device.

The torque about the pivot point of a single exert door can be reasonably modeled as:

$$\tau_{door} = K_{eff}\Delta\theta \tag{2-14}$$

where K_{eff} is the stiffness of one exit door mechanism (ex. a torsion spring constant or a stiffness of a deformable body) and $\Delta\theta$ is angular displacement of the exit door about its pivot. Through a torque balance about the pivot point of the doors, the output force can be estimated as:

$$F_{out} = \frac{2\tau_{door}}{l\cos\theta} = \frac{2K_{eff}\Delta\theta}{l\left(\frac{h}{l}\right)} = \frac{2K_{eff}\cos^{-1}\left(\frac{h}{l}\right)}{h} \tag{2-15}$$

where h is as defined in Figure 2-9 and l is the length of the exit door. Note that the output force is multiplied by 2 in the above formula because there are two identical exit door mechanisms contributing torque that is counteracted by the output force.

In one iteration of the device, the exit door mechanism consisted of rigid doors with four identical torsion springs acting at the pivot point. 90-degree torsion springs were chosen which had the smallest, commercially available size and spring constant. From the data sheets, the maximum torque provided by the springs is 0.05 in-lbs, corresponding to K_{eff} = 2(3.56) = 7.12 mN-m/rad. Using h = 1.94mm and l = 3.30mm as designed, this corresponds to a maximum output force of approximately 7.0 N. The different exit door configurations are discussed in section 2.3.

Combining this estimate for output force with the results from Figure 2-6, this yields a minimum motor torque of approximately 60 N-mm. The Pololu motor (700:1 sub-micro plastic planetary gearmotor 6Dx21L mm, part no. 2359) implemented in this prototype has a stall torque of approximately 80 N-mm. This comparison indicates that the motor provides sufficient torque to drive the designed four-bar linkage mechanism, even at the point where the linkage requires the maximum amount of torque.

Evaluation of Concept

The pushrod concept demonstrates many advantages over the rotating disk concept and addresses many concerns revealed through testing of the rotating disk concept. First, this concept now incorporates a mechanism, which does not rely on gravity, for forcing pill release from the device. The pushrod mechanism also allows for the same form factor as the rotating disk concept, in that the pills are loaded along the length of the device, and the mechanism acts primarily along the diameter of the device. Second, this concept allows motor power to be transmitted more efficiently. The motor now functions to generate pushing force to release the pill, whereas the motor previously functioned primarily to overcome friction. Third, motor control is slightly simplified with this concept. Just as with the rotating disk concept, the motor functions unidirectionally. However, with the pushrod concept, the motor can operate continuously (i.e. the motor completes one full rotation without stopping), whereas with the rotating disk concept the motor may need to stop to allow time for the pill to exit the device.

The pushrod concept also has an increased number of moving parts relative to the rotating disk, introducing the potential for unanticipated failures and jamming. The device must be implemented such that the modeled motions (i.e. planar and rigid) are met. Otherwise, the concept may fail to achieve pill release as intended.

2.3 Material Selection and Manufacturing Methods for Pill Release Mechanism

Linkages

Linkage dimensions were determined from a balance between the dynamic requirements detailed in section 2.2 and material stability which becomes problematic at the small sizes imposed by the size constraints of the device. The linkage lengths used in the final iteration of the device are given in Figure 2-6. The shapes of the drive link and connecting links are given in Figure 2-10. Distance between the edges of holes and the edges of the part was maximized as much as possible to prevent part material failure. The push link shape is also shown in Figure 2-10(c). Its length is not determined in the dynamic calculations in section 2.2, but instead by geometric constraints to ensure it does not impede pill loading when retracted and extends far enough to push pills passed the exit doors.

One important assumption in the model in section 2.2 is that motion is in the out-of-plane direction is negligible. To minimize out-of-plane motion, linkages were connected using screws. Holes in the drive link and push link were threaded to secure the screws, while holes in the connecting link were through holes to ensure frictionless rotation of the linkages. The screw heads allowed the linkages to be lightly pressed together, but not so much as to introduce extra friction at the interfaces. A small amount of adhesive was placed at the bottom of the threaded holes to prevent the screws from loosening during operation.

The push link in the device was created using a Formlabs SLA 3D printer and the screw hole was tapped by hand after printing. 3D printing was chosen due to the slightly complex shape as well as the presence of the chamfer as discussed in section 2.2. The chamfer angle was chosen as $\theta = 45°$ based on the analysis in the previous section. The final design is shown in Figure 2-10(d).

The drive and connecting links were also fabricated using a Formlabs printer in order to reduce active manufacturing time. Through holes were hand tapped after printing. However, the parts were designed to be accessible to other forms of manufacturing, such as laser cutting, since the features are mostly planar. This choice was made in case other materials needed to be explored to increase strength of the parts.

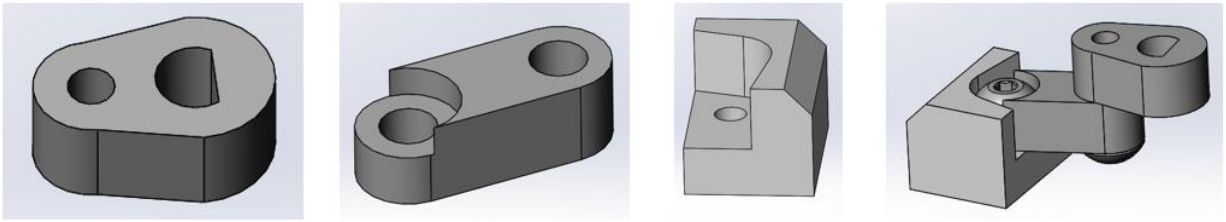

Figure 2-10: Shapes of (a) drive link, (b) connecting link, and (c) push link used in final design of prototype. (d) shows how the parts are joined and interact in assembly. The mechanism is driven by a motor at the D-shaped hole in the drive link. Linkages are secured by screws and rotate freely.

Exit Doors

Exit doors are necessary to keep pills from leaving the device in an uncontrolled manner (for example, rolling out of the opening without the pill release mechanism being triggered). Two different forms of exit doors were considered for the final design as shown in Figure 2-11. The first form consisted of a rigid exit door which rotates about a hinge and is nominally closed by action of torsion springs. The second form consisted of a flexible exit door made of highly (elastically) deformable material which acted as a one-piece barrier to prevent unanticipated pill release.

Due to the complex geometry of the rigid exit doors and the very small features, a Formlabs SLA 3D printer at high resolution was used to create the doors. The torsion springs were mass produced and ordered from McMaster Carr (part no. 9271K576 and 9271K644).

The rigid exit door configuration was used in the bench level proof of concept prototype. Their main advantage was to provide reliable and powerful ejection of the pills from the device. However, in the in vivo prototype there is not enough space for the rigid exit doors due to the size of the dowel pins and torsion springs. In addition, the size of these parts also made assembly of the device very difficult and unnecessarily added time to the manufacturing process due to the required small features for the interface on the bottom housing part. It was therefore necessary to explore alternative configurations for the exit doors, leading to the flexible exit door form.

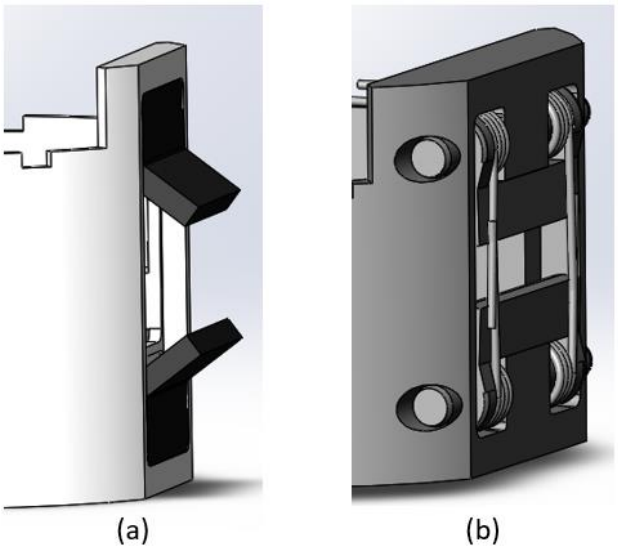

Figure 2-11: Two configurations for the exit doors considered during the design of the device. (a) flexible exit doors, shown in its extended position. (b) rigid exit doors with torsion springs, fixture to the housing with dowel pins.

The flexible exit doors required a material that could experience large, elastic deformations without excessive stresses. With such a material, the material could deform similarly to the rigid exit doors without the need for torsion springs and without risk of tearing. A silicone rubber made from FDA-listed materials and produced by McMaster Carr (part no. 86045K94, 60A durometer from McMaster Carr) was used to create the flexible exit doors. The silicone sheets were laser cut and adhered to the device using a Loctite M-21hp medical device epoxy adhesive. Only the bottom part of the door was adhered, while the top half was free to deform when force is applied to the end, acting like a hinge to allow pills to leave the device when the pill release mechanism is acting.

3. Design of Electronics and Control for Pulsatile Release

3.1 Actuation and Control Strategy for Pill Release Mechanism

Control Strategy Concept

The pill release mechanism is controlled by a small (6mm in diameter by 21mm in length) geared direct current (DC) motor supplied by Pololu (part no. 2359). Because the motor does not have any built in encoders, the pill release mechanism was designed to have a very simple control scheme. The four-bar linkage functions such that a single rotation of the drive link corresponds to a single cycle of linear reciprocation at the push link (i.e. a forward motion and a return motion). Therefore, one rotation of the motor corresponds to one pill being released from the device. It should also be noted that precise angular positioning of the motor is not necessary to achieve satisfactory pill release with this strategy.

The device was designed to hold and release at least five pills over five days. Because of the low number of cycles which the device must perform during in vivo testing, control of the motor was performed open-loop with a series of on-off cycles. That is, the motor is turned on for a precisely measured and optimized amount of time, allowing the push link to release a pill and retract, then is turned off for a specified amount of time corresponding to the period between dosing.

The on-off control of the motor is triggered using a metal-oxide semiconductor field-effect transistor (MOSFET) with a control signal supplied by the device's microcontroller. A schematic of the electrical signal and power flow is shown in Figure 3-1. The microcontroller controls timing of the digital signal, while power flow to the motor is provided separately from batteries. When the microcontroller sends a digital "HIGH" signal to the MOSFET, current is allowed to flow directly from the batteries to the motor with very little current required from the microcontroller.

During bench level testing, the motor actuation was triggered manually using a mechanical switch in place of the MOSFET shown in Figure 3-1.

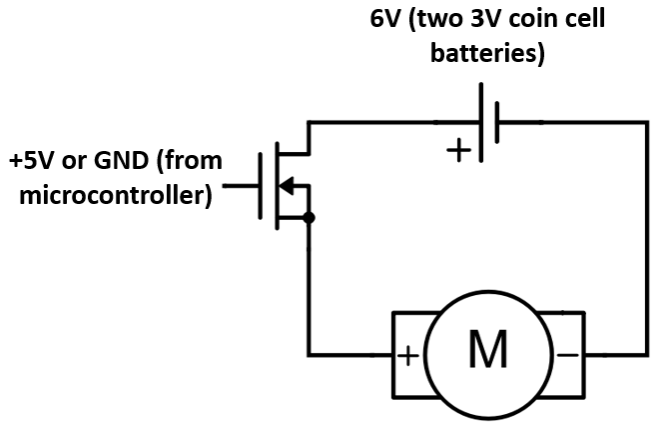

Figure 3-1: Circuit schematic of illustrating how the pill release mechanism's motor is controlled. A digital signal from the microcontroller with precise timing is supplied to the MOSFET. When the digital signal turns on, current flows from the batteries to the motor to actuate it.

Optimization and Reliability Testing of Open-Loop Control Strategy

As discussed in previous sections, the torque load required by the motor is a complex function of output force, linkage geometry, and supplied current from batteries. To complicate matters, the output force may generally vary as at any given angular position due to forces that cannot be modeled reliably (such as friction). Because the speed at which a DC motor rotates is directly affected by the load applied to it, the time required for the motor to complete one revolution cannot be accurately predicted. At the same time, the mechanism is relatively insensitive to rotational position; if the motor rotation overshoots by 10 degrees, it is unlikely to affect the device's overall goal of dispensing a pill. Therefore, open loop control may be sufficient to control the device for a low number of doses, eliminating the need to include sensors and complex feedback control.

If the mechanism were to fail, there would be two macroscopic failure modes as the device relates to pill dispensing. The device may overdose if the mechanism rotates too far and releases extra pills. The device may also under-dose if the mechanism does not rotate far enough and fails to release a pill. These failure modes can be used to set up a test that assesses the device's reliability over many doses and empirically determines an operating point for the motor's open-loop control.

The general outline for such a test is as follows:

1. Assemble the device exactly as would be used in vivo.
2. Program the controller to run the motor for a known, specified amount of time.
3. Allow the device to dispense pills until a failure mode (under-dosing or overdosing) is observed.
4. Record the number of pills successfully released before the failure.

Repeating this procedure over a wide range of motor run times is expected to produce an empirical curve similar to that shown in Figure 3-2. At run times that are far from the ideal operating point, the number of successful releases is expected to be near zero. As the device reaches the ideal operating point, the number of successful releases is expected to increase until it reaches a maximum. As long as the number of successful releases is well above the number of pills to be released during in vivo studies over many repetitions, the motor can be assumed to be reliable for sustained release studies.

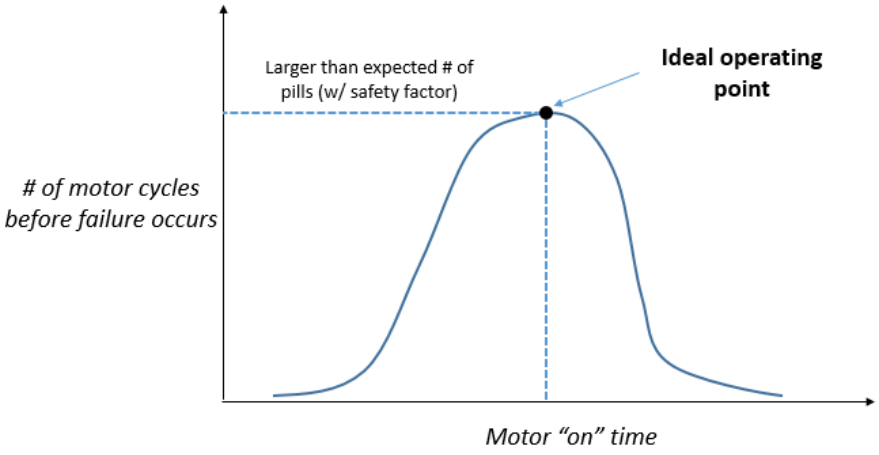

Figure 3-2: Predicted motor optimization curve, plotting commanded motor "on" time to the number of successful cycles before the mechanism experiences a failure. The ideal operating point corresponds to the motor timing that will be used in vivo.

Future work will focus on executing this test in order to optimize motor function for reliability during in vivo testing.

3.2 Power and Hardware Components

Choice of Microcontroller and MOSFET

For the bench level testing of the motor control scheme, an Arduino Uno was used as the microcontroller. Arduino is easily programmable and pins are easily accessible for rapid electronics prototyping. An IRF520 power MOSFET was used with a breadboard to test the motor control along with batteries (discussed in the next section).

For the in vivo prototype, an ATmega328 microcontroller (part no. ATMEGA328PB-AUR from Digikey, Inc.) was chosen to control the device. Its compact size (8.75mm x 8.75mm x 1.20mm) allows it to fit easily within the device. During operation, the microcontroller can pull approximately 12 mA. When it power-down mode, it uses a maximum of 15 μA. This power consumption is sufficiently low to allow long-term residence battery drainage.

Power Management: Choice of Batteries

Due to the use of a DC motor for actuation and a microcontroller for control, batteries were chosen as the type of power supply for this device. Coin cell batteries were used in the final implementation of the device due to their compact size, reliable manufacturing, and availability in a variety of specifications. One consideration with coin cell batteries, however, is the tradeoff between size and capacity. Batteries must be small enough to fit within the device but be capable of supplying enough current for the motors. The motors used in this device have a stall current of 400 mA and operating current at maximum power output of approximately 220 mA.

In the final design, the device used Energizer 675 coin cell batteries (part no. AZ675DP-8 from Digikey, Inc.) which are commonly used in hearing aids. The batteries have an operating voltage of 1.25V to 1.4V and a capacity of 620 mAh. Therefore, four batteries were placed in series to achieve an acceptable output voltage for the motor. In this configuration, the battery pack has a total diameter of approximately 11.4mm, a total height of approximately 20mm, an operating voltage of approximately 5V, and a maximum output current of 620 mA. These specifications were found to be sufficient to operate the motor during bench level testing. Furthermore, because the motor has a stall current of 400 mA, the onboard electronics can draw as much as 220 mA before current supply to the motor becomes affected. A significant margin is left to power onboard electronics with little concern of insufficient current supply when the transition is made to an in vivo prototype.

Component Organization in Device

For bench level testing, large-scale components were used to confirm functionality of the motor control circuit. Components were connected with for ease of prototyping and troubleshooting. The coin cell battery pack was created using electrical tape and was placed outside of the device during bench level testing.

For the in vivo prototype, further scale down and organization is necessary to ensure that all components fit compactly into the device. Future work is focused on designing a custom PCB for placement of the ATmega328 microcontroller and MOSFET as well as providing reliable connections for the battery and motor.

4. Design of Device Housing: Material Selection and Backflow Prevention

4.1 Housing Components and Manufacturing Methods

There are two main parts which make up the device's housing, each requiring a different manufacturing process due to differing feature complexity and required precision. The bottom housing part is where exit doors attach to the device and where the push link reciprocates when the pill release mechanism is active. The upper housing part is significantly longer and contains a column to house the store pills and a column to secure the device's motor. The two parts are aligned using precisely placed alignment grooves and secured using medical epoxy adhesive.

The upper housing part was fabricated using a Formlabs 3D printer with a biocompatible dental resin. 3D printing was necessary for this part because its length and very small features make it difficult to safely and effectively machine the part. 3D printing also helps decrease total active manufacturing time and time between iterations.

The bottom housing part was designed to be machined because many clearances needed to be precisely controlled to interact with the push link motion. Furthermore, machining the part helps reduce cost because 3D printing would require large volumes of resin for space that is not functional. ABS plastic was chosen as the material for the bottom housing part because it is easy to machine, inexpensive, resistant to chemical attack by gastric acid, and biocompatible. Machining was done using a benchtop CNC Othermill and operations were created using HSMWorks for Solidworks.

Both parts were designed to have diameters strictly less than 15.8mm (5/8 inch) in order to fit through the largest overtube available for in vivo testing. Clearance was included in the design so that each part had a diameter of 15.3mm.

4.2 Backflow Prevention Strategy

Backflow prevention is a very important consideration for this device for many reasons. First, the device contains many sensitive parts on its interior which may be less chemical resistant than the housing. For example, the motor used in the device is constructed of metallic components which would degrade quickly when exposed to acid. Degradation of such components could lead to unsafe conditions for the patient or loss of functionality of the device. Second, it is necessary to protect unreleased pills in the device from exposure to gastric acid. Degradation of unreleased pills from acid exposure could lead to medication overdosing or reduced treatment efficacy.

The most common solution for preventing fluid backflow is the use of a duckbill valve. This valve relies on a fluid pressure differential to allow fluid flow in only one direction. For this particular application, however, a duckbill valve would not be viable to prevent backflow. These valves require that a high pressure fluid is expelled from the valve towards a lower pressure fluid. In this device, it is a solid object (i.e. a pill) which we are expelling from the device into a fluid. The use of a duckbill valve would either introduce unnecessary amounts of friction (in the case where the pill size is very close to the valve's opened size) or cause fluid to enter to flow into the device due to the lack of pressure inside the device.

An alternative backflow prevention strategy for this device was explored which uses an oil-based substance to block acid flow. While the device consists of many solid components, from motors to pills, there are many open cavities in the device which can be filled with oil to surround and protect the solid components. The oil in the substance would be sufficient to prevent acid (which has a high water content) from passing into the device. If the oil were of high enough viscosity, it could be contained within the device through surface tension and other resistive components such as a spring-loaded door.

Instead of modeling the interaction of oil-based substances and acidic fluids, this strategy was explored empirically in parallel with durability and material selection of the device's housing. Vaseline (a petroleum jelly) was the chosen substance because it is commercially available, meets biocompatibility and safety standards, and known to be highly viscous. In addition, the principle behind which Vaseline helps moisturize skin is similar to this backflow prevention strategy: it retains moisture by blocking the evaporation of water from the skin.

It should be noted that other fluids were considered for the backflow prevention strategy. Namely, baby oil was considered as an alternative due to its low viscosity. However, baby oil is difficult to retain in the device over long periods of time with proper sealing. Because this device has a non-negligible gap between the exit doors, baby oil may flow out of the device over time and reduce the device's ability to prevent backflow. Vaseline was advantageous because it has a lower viscosity when heated (during assembly) and then becomes more viscous after cooling, preventing the fluid from leaking during residence. In principle, the fluid could be optimized in future work to explore other oily substances that balance the need to retain fluid during residence while reducing fluid resistance that may hinder the pill release mechanism.

4.3 In Vitro Testing of Device Housing and Backflow Prevention

To test the housing's resistance to chemical attack and assess viability of the described backflow prevention strategy, a number of experiments were conducted which involved simulated gastric fluid (SGF). In the full-scale test, the device is completely assembled in a "stripped down" state and placed into SGF. The housing (including the exit doors) was joined as in the normal design of the device, and the housing was filled with Vaseline. However, the assembly did not contain functional components such as the motor, linkages, or pills. This test evaluates the device's overall response to an acidic environment and ability to prevent acid flow into the device. In the control test, each component of the device was placed into SGF in an unassembled state. This test evaluates each individual component's response to the acidic environment and can help identify failure points in the device's assembly.

Both tests were conducted with the following procedure after the parts or assembly were prepared for testing:

1. Place device into flask or other container
2. Fill the container with enough SGF to completely submerge all parts.
3. Place the container into a shaker and set the temperature to 37 degrees Celsius to mimic environment of stomach.
4. Allow the device to remain in test configuration for one month, checking periodically for major chemical corrosion failures.
5. Remove the device from the fluid and examine the steel dowel pins. Take measurements of their lengths and diameters to quantitatively assess whether the device has failed to prevent backflow. Also make note of any discoloration that may occur on the stainless steel, or other interesting features on the device.

To quantitatively assess acid backflow in the full-scale test, two stainless steel dowel pins were placed in specific orientations and locations as shown in Figure 4-1. This strategy was chosen because most electronic sensors for detecting pH or moisture may be damaged at concentration of acid used in this test. Because stainless steel is known to be much more sensitive to strong acids than many plastics, any degradation of the steel would indicate acid inflow even if no damage were observed to the housing components. These particular orientations and locations were chosen to

best characterize acid dispersion through the Vaseline in the case where acid is able to flow into the device. The pin represented in red helps characterize acid dispersion through the pill holding column, which would indicate contamination of unreleased pills. The pin represented in blue helps characterize acid dispersion in the direction of major function components of the pill release mechanism, including the motor and linkages. The diameter and length of the pins were measured at the beginning and end of the test with the results shown in Table 4-1.

It should be noted that the dimensions of the parts did not change significantly during one month in SGF. Furthermore, none of the plastic or 3D printed parts showed any visible sign of distortion in either the full-scale or control test. However, it should be noted that the dowel pins in the control test (which were exposed directly to SGF) showed significant discoloration and were black in color. The same dowel pins in the full-scale test showed no such discoloration, indicating that SGF did not flow into the device in significant enough quantity to affect the stainless steel.

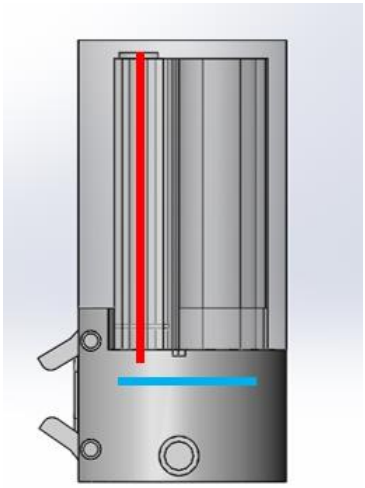

Figure 4-1: Dowel pin placement for durability tests. One long stainless steel dowel pin (red) is oriented along the pill holding column and indicates acid dispersion along the column. The other, shorter dowel pin (blue) is placed near the device's exit hole and oriented along the diameter of the device and indicates acid dispersion into the device in the direction of key functional components.

Dowel pin in pill holding column (red in figure)

	Control Test	*Full-Scale Test*
Diameter – Initial (mm)	1.51	1.50
Diameter - After 1 Month (mm)	1.52	1.51
Length – Initial	1.51	19.96
Length – After 1 Month (mm)	1.52	19.96

Dowel pin along device diameter (blue in figure)

	Control Test	*Full-Scale Test*
Diameter – Initial (mm)	1.51	1.51
Diameter - After 1 Month (mm)	1.51	1.52
Length – Initial (mm)	12.05	12.04
Length – After 1 Month (mm)	12.02	12.03

Table 4-1: In vitro test results for housing durability tests. For each dowel pin, the diameter and length were measured before and after the test to quantitatively measure whether the interior of the device was exposed to acid.

4.4 Increased Drug Loading: Multiple Pill Holding Columns

Overview of Concept

The initial drug loading requirement for this device was to hold 30 individual pills, corresponding to one pill per day for one month of operation. In section 2.2, the advantages of loading the pills in a column in the specified orientation were discussed as this strategy related to mechanical functionality and drug capacity of the device. However, even with this strategy, a single column of 30 pills would require that the device be over 5 inches in length. A device of this length would have many problems including difficult in administration to the stomach as well as reduced reliability in part manufacturing. In addition, the device would use available interior

volume inefficiently because the upper capsule would have a very large, unused cavity adjacent to the column of pills.

A feature to improve space efficiency in the housing of the device was conceptualized which involves the use of multiple pill holding columns that feed into a single column for loading into the release mechanism. This feature makes use of the pills' ability to roll as well as springs with different spring constants. The feature functions as shown in Figure 4-2 and has the following main steps:

- The pill loaded into the pill release mechanism is expelled from the device with the mechanism detailed in section 2.1.
- The pills in column 2 (right) have a spring with a higher spring constant/force than in column 1 (left). The pill within this column will be forced between two pills in column 1.
- All of the pills in column 1 will shift downwards due to the spring in the column. This occurs because the pills will be at an unstable equilibrium with the pill in column 2.

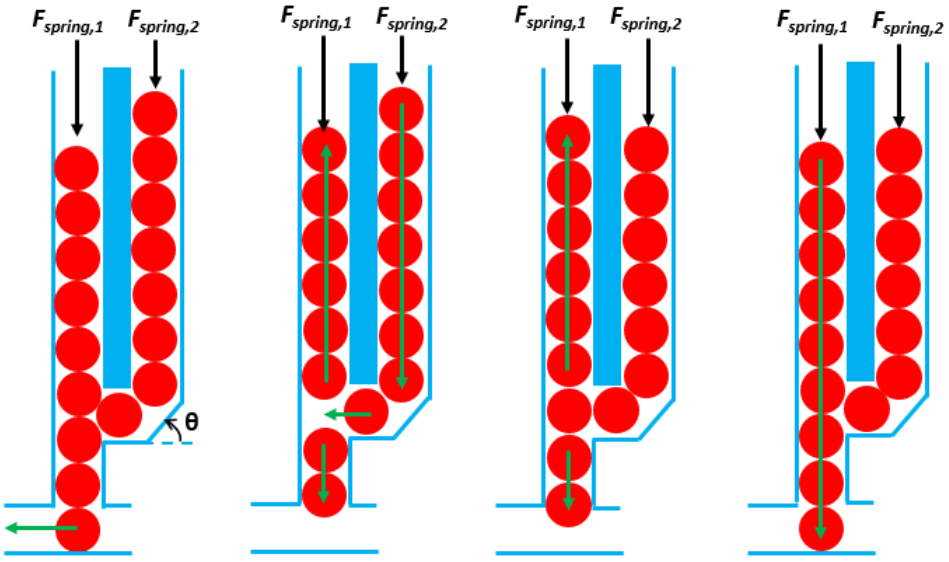

Figure 4-2: An overview of pills interacting with the two pill holding columns. Pills in column 2 (right) are subject to a larger spring force than column 1 (left), allowing for the diagrammed motion. Green arrows show the direction of motion of the underlying pills at each step. Regions in blue indicate rigid features on the device's housing.

Design of Column Springs

The use of multiple columns relies on springs with two different but carefully chosen spring constants. The spring in column 2 is necessary to force the pills in the column into column 1, which feeds into the pill release mechanism. The spring in column 1 is necessary to ensure pills continue to be loaded into the pill release mechanism regardless of the device's orientation (i.e. loading into the pill release mechanism does not rely on gravity).

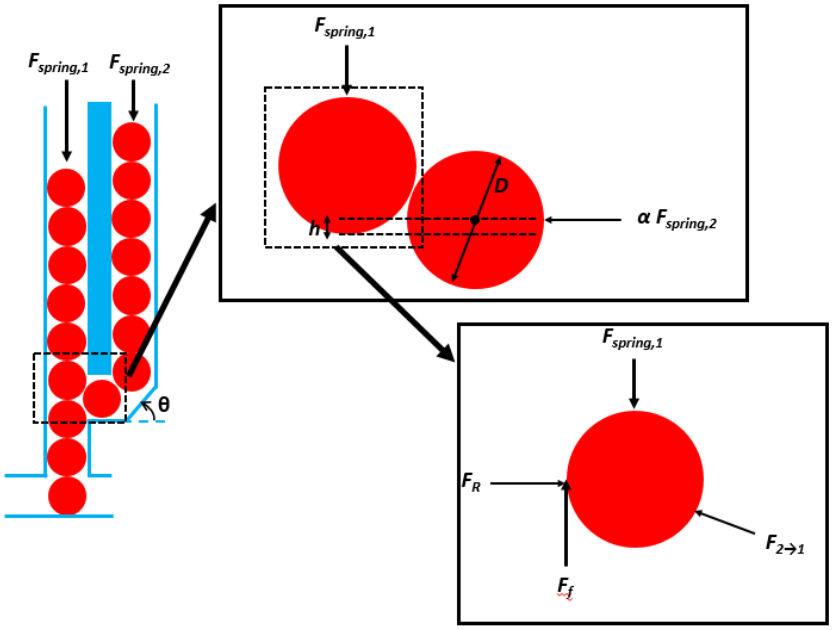

Figure 4-3: Free body diagram of pill interaction in the two-column increased drug loading strategy. A parameter h is introduced to account for relative pill offset due to manufacturing imperfections. F_R is the reaction force of the pill in column 1 on the housing wall, F_f is the corresponding friction force, and $F_{2\to1}$ is the interaction force between the two pills.

A schematic of this form of loading is shown in Figure 4-3. From the free body diagrams shown, it is possible to relate the relationship between the spring forces as a function of pill and loading geometry. Assuming the pills are the same diameter:

$$\frac{F_{spring,1}}{\alpha F_{spring,2}} = \frac{\frac{1}{2} - \frac{h}{D}}{\sqrt{1 - \left(\frac{1}{2} - \frac{h}{D}\right)^2}} - \mu \tag{4-1}$$

where F_{spring} is the corresponding spring force, D is the diameter of the pills, h is the offset of the pills as shown in the figure (corresponding to manufacturing imperfections that may not be negligible), and μ is the coefficient of friction between the pills and the column wall. A factor α is also introduced which reflects the fact that the spring force in the second column may not be perfectly transmitted. This transmission inefficiency will be due to the fact that the pills in column 2 load against an inclination (as depicted in Figure 4-3).

Because this device ultimately did not require a large enough number of dosages to necessitate a second column of pills, this model was not tested extensively. However, the calculations above indicate that if the manufacturing of the housing can be done reliably enough to minimize the offset h, springs with reasonable constant can be incorporated in the design to allow a greater number of pills to be fed to the release mechanism without the need for an additional actuator.

5. Design of Retention Mechanism

5.1 Concept for Retention

After the device is administered in the stomach, it must be able to be retained when subjected to a certain force associated with peristalsis near the pylorus. A common retention mechanism, introduced in previous work conducted by Bellinger et al, is to have highly elastic arms which can fold during administration but expand once delivered to the stomach. These arms function by changing the effective diameter of the device during and after administration.

A similar idea was implemented and tested with this device. In the star device developed by Bellinger et al, the arms served as both the housing for the device (to load drug) as well as the retention mechanism. In this device, the arms are exclusively used for retention. The arms are made of a highly elastic material, such as a rubber, so that the arms can undergo very large deformations while folded and elastically return to their extended position after administration. Figure 5-1 schematically depicts this strategy.

One design consideration is the cross section and size of the arms. The cross sectional size is related to how resistant the arms will be to deformation; the larger the cross-sectional dimensions, the greater the resistant to deformation (in general). The arm length is related to the size of the pylorus; longer arms are needed for larger pyloric openings. At the same time, longer arms tend to experience much larger deflections than shorter arms, which can reduce resistance to pyloric passing.

As a first approximation, the length of the arms can be determined geometrically. Assume there is some angular spacing between each arm and that each arm has identical length. Geometrically, the smallest linear spacing between any two arms (as measured from their ends) must be greater than the pyloric opening (see Figure 5-1). Using the law of cosines, the minimum value for l_{arm} can be approximated as:

$$l_{arm} = \frac{D_{pylorus}}{\sqrt{2(1-\cos\theta_{min})}} - \frac{D}{2} \tag{5-1}$$

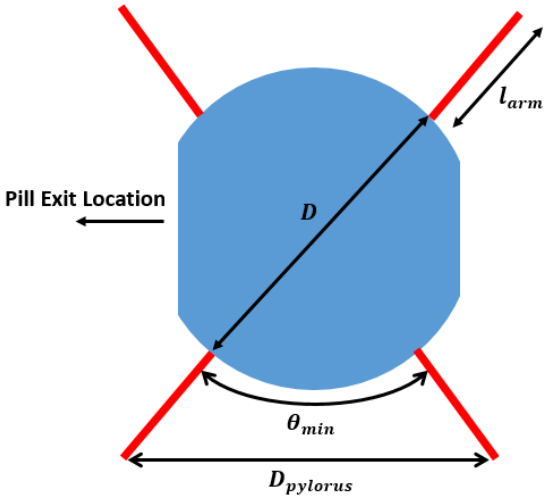

Figure 5-1: Schematic of the retention arms relative to the shape of the device. Retention arms are shown in red, while the device's housing is shown in blue. l_{arm} denotes the length of the arm measured from the body of the housing, D denotes the diameter of the device's housing, θ_{min} corresponds to the angle between the pair of arms that are spaced closest together, and $D_{pylorus}$ is the diameter of the pyloric opening.

5.2 Manufacturing Methods

The material commonly used for retention arm designs and was readily available for use in the lab was Elastollan 1185A10. To create retention arms out of this material, a mold is first created out of PDMS using 3D printed positives of the desired arm geometry. The parts are then manufactured using a compression molding process. The mold is filled with solid Elastollan pellets and heated with a heat gun until the pellets melt. Once the pellets are melted, a piece of heavy aluminum is placed on top of the mold and compressed while the Elastollan cools.

In the device's housing, pockets are milled that fit part of the length of the molded arms. The pocket is extended along the length to allow the arms to fold into the device while being administered, to keep the diameter of the device under 15.8mm. The molded arms are secured to the device using epoxy. CAD models of the arms in the extended and folded states are shown in Figure 5-2 and demonstrate how the arms interface with the device housing.

Figure 5-2: CAD models demonstrating the form factor of the retention arms in the (a) extended, and (b) folded states. Pockets are milled into the housing to allow the arms to be securely fixed while extended and fully collapsed into the housing while folded.

5.3 Experiment to Determine Arm Design

Rubbers (such as the Elastollan used in this concept) typically have highly nonlinear stress-strain relationships which require material testing and computationally intensive simulations to predict behavior when subjected to high strains. Because the geometry of the retention arms was more of less fixed in order to reduce manufacturing complexity and incorporate biocompatible design, the dimensions of the arms were confirmed experimentally.

Arms with a 3mm diameter, semicircular cross section were manufactured using the process detailed in section 5.2. Each type of arm was then positioned into a test fixture which replicates how the arms would be installed and function during in vivo testing (see Figure 5-3). The "funnel" test as used in the design of the star device by Bellinger et al was replicated [13]. The fixture was placed in a funnel with diameter 18mm and a force was gradually applied and measured using an Instron machine. This orientation for the fixture was chosen because this is the direction in which the retention arms have the lowest resistance to deformation. The fixture was compressed until the force on the fixture reached a maximum and then began to drop, indicating that the force was large enough to deform the rubber arms to the point that the device's overall diameter is less than 20mm.

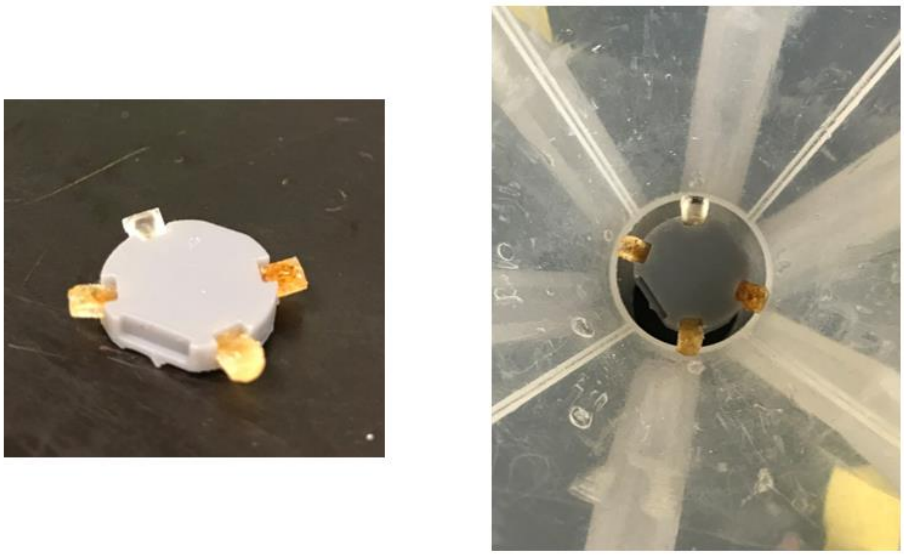

(a) (b)

Figure 5-3: Retention arm test fixture using the funnel test devised by Bellinger et al. (a) 3D printed housing fixture with the molded Elastollan arms. (b) Housing fixture with molded arms placed inside of a funnel with 18mm diameter. Force was applied in the direction perpendicular to the plane of the page.

The force measurements are shown below in Table 5-1. The average peak force required to force the fixture through the funnel was 4.04N with a sample standard deviation of 0.65N. With these statistics, a 95% confidence interval for the average peak force is [3.14, 4.94] N. This test indicates that, with 95% confidence, the chosen configuration for the retention arms will withstand peristaltic forces in the pylorus of greater than 3N, which was the design requirement for the arms.

Trial	1	2	3	4	5	**Overall**
Force (N)	5.0	4.4	3.5	3.5	3.8	4.04 ± 0.65

Table 5-1: Force measurements for retention arm design test

The results from this test indicate that the chosen geometry is acceptable for resisting pyloric peristalsis. In the final design of the retention mechanism, the cross section of the arms will be kept the same, but the arms will be extended slightly to overcome geometric consideration discussed in section 5.1. From the device's design, D = 15.3mm, $D_{pylorus}$ = 20mm, and θ_{min} = 70°. Therefore, the arms need to be approximately 9mm from the housing's surface for effective retention.

6. Conclusion

This project was dedicated to demonstrating proof of concept of a novel device for controlled drug delivery using an electromechanically driven mechanism. With this pill release strategy, the goal was to achieve pulsatile pill release. That is, pills are released to the stomach environment at discrete points in time rather than delivering medication through continuous release.

The development of this device was modular, consisting of many separate design areas that needed to be precisely controlled to ensure functionality. The most critical module was the pill release mechanism. Two different concepts were explored, and the concept ultimately developed in detail involved a pushrod driven by a motor using a linkage that converts rotary motion to linear motion. The dimensions of the linkage needed to be carefully chosen to balance manufacturing limitations, material stability, size constraints, and motor specifications. In addition to the pill release mechanism, the device needed to have a biocompatible housing which holds the unreleased pills, release mechanism, and electronics. A housing with a capsule-like form factor was designed which used the length of the device for storing components despite the strict diametric restriction on the device. To protect the device interior, a strategy for backflow prevention was explored in which Vaseline filled the interior of the device and the exit to impede gastric acid flow.

Through this development process, a prototype was created which successfully demonstrates many of the design requirements set forth by this project. A picture of this prototype is shown in Figure 6-1. This iteration of the device is approximately 20mm in diameter and approximately 60mm in length. The device is capable of holding and dispensing approximately 6 pills; cylinders of acrylic were used to mimic pills during bench level testing. The pills release with no outside intervention from the mechanism. During testing, the motor was attached electrically to a mechanical switch, and pressing the mechanical switch triggered motor rotation and pill release. The mechanism successfully released six pills only as the result of switch presses, which is analogous to an electrical signal being sent by the Arduino.

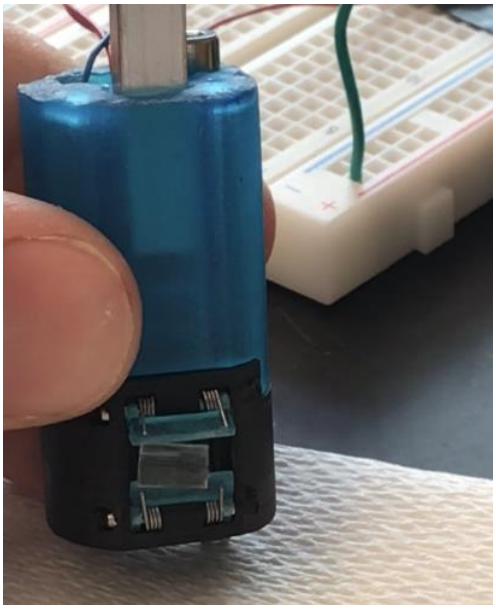

Figure 6-1: Functional bench level prototype of pulsatile pill release device. In this iteration, the device is self-contained. The motor is driven by external electronic components for proof of concept. The motor is also actuated manually with a mechanical switch rather than controlled by an Arduino completely. This prototype holds and dispenses approximately 6 pills and is approximately 20mm in diameter.

A number of modules are still in development and are areas of future work. A concept for a retention mechanism was conceived based on previous work by Bellinger et al. The concept involves highly elastic arms which can be retracted into the device during administration and expand upon entering the stomach. These arms create an effectively larger diameter for the device to prevent passage into the pylorus during in vivo testing. Onboard electronics also need to be incorporated to make the device self-contained and autonomous for functionality during in vivo testing. After the successful implementation of all concepts, the device will be tested in vivo to demonstrate proof of concept of the pulsatile controlled drug release in a more clinical environment.

7. Appendices

Appendix A: Pin Joint Friction for Four-Bar Linkage Concept

In previous analyses, it was assumed that the friction between the pin joints and the links was negligible. However, this assumption may not always be valid depending on the materials used and the magnitude of the reaction forces experienced between the links. Additional analysis was performed in which it was assumed that friction in the pin joints could modeled as an additional torque acting at the pin joints:

$$\tau_f = \mu_J \, |R_{net}| \, \frac{D}{2} \tag{A-1}$$

where τ_f is the torque on the joint due to friction at the pin joints, μ_J is the coefficient of friction between the pin joint material and the link material, and *D* is the diameter of the pin joint.

The assumption of frictionless joints can now be relaxed by modeling a frictional torque acting at the pin joints between links 1 and 2 and between links 2 and 3. The relationship between input torque and output force can be adjusted such that:

$$\frac{\tau}{F_{out}} = l_1 \left[\sin\theta_1 + \cos\theta_1 \left(\frac{h + l_1 \sin\theta_1}{\sqrt{l_2^2 - (h + l_1)^2}} \right) \right] + \frac{sign\left(\dot{\theta}_1 \cos\theta_1\right) \mu_J \left(\frac{D}{2}\right) l_2}{\sqrt{l_2^2 - (h + l_1)^2}} \tag{A-2}$$

From this analysis, it is shown that the effect of pin friction can be modeled as an additional term in the torque-force relationship from equation A-2. In addition, this term is proportional to the product of μ_J and *D*. Because $D \ll l_1, l_2, h$ and $\mu_J \ll 1$, the second term is much smaller in magnitude than the first term. Therefore, from this analysis it is reasonable to within first order approximation to neglect any effects due to friction in the pin joints.

Appendix B: Friction Test with Formlabs Resin Material

In many of the models discussed in this thesis, friction is not necessarily negligible and affects the functionality of the device. Specifically, both concepts for a pill release mechanism were shown to contribute significantly to the input power required by the motor. In order to have a more accurate estimate of friction, a friction test was developed and corresponding fixture was designed.

A schematic of the test and the corresponding fixture is shown in Figure B-1. Two test specimens, made out of the material of interest, are placed between a rotating plate and a fixed plate. A lever arm (shown in red) is connected rigidly to the rotating plate. As force is applied to the lever arm, the rotating plate will also begin to rotate once the torque on the plate is large enough to overcome the torque applied on it by the frictional forces between the test specimen and the fixed plate. A known normal force applied to the top plate induces a friction force at the test specimens which are proportional to the coefficient of friction. By measuring the normal force on the rotating plate and the force applied to the lever arm, the coefficient of friction can be estimated. Figure B-1 also shows a free body diagram of the top, rotating plate. Through a sum of torques on this plate, a relation to estimate coefficient of friction of the test material (μ) can be found:

$$\mu = \frac{F_{applied}}{F_N}\frac{l_{arm}}{R} \tag{B-1}$$

where $F_{applied}$ is the force applied to the lever arm, F_N is the total normal force applied to the top plate, l_{arm} is the length of the lever arm, and R is the distance between the center of the plate and the center of the test specimens.

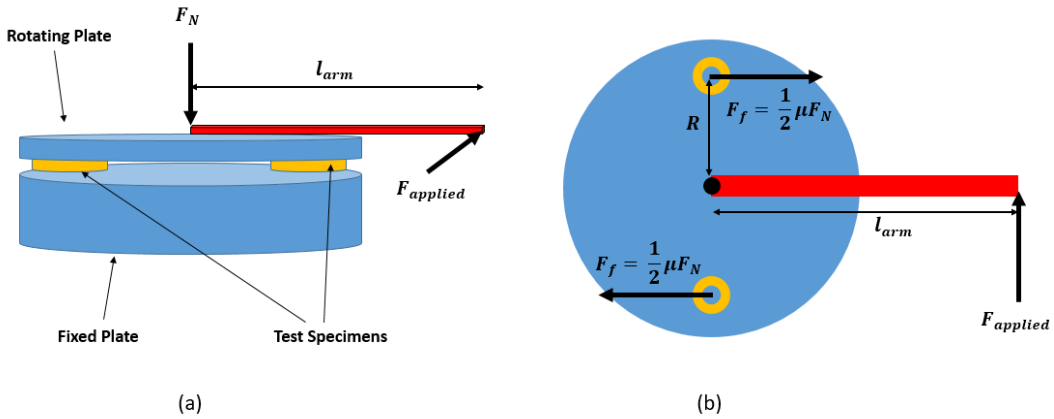

Figure B-1: Schematic of the friction test and the test fixture used to for measurement of coefficient of friction. (a) A high level overview of the test. Two circular two specimens are placed between two plates. One plate, which is connected to a lever arm (red), is free to rotate and is mated with the test specimens. The other plate is fixed. Measured forces are applied both to the top surface of the rotating plate and to the end of the lever arm. (b) A free-body diagram of the top plate.

A picture of the test fixture is shown in Figure B-2. Several design principles were incorporated to ensure that the test fixture was properly controlled and did not incorporate confounding variables. The rotating plate is connected to the lever arm through a shaft that is mounted in a ball bearing. The ball bearing ensures that all of the torque applied from the lever arm goes into rotation of the plate instead of overcoming rotational torque introduced by the fixture. Furthermore, an additional plate was introduced above the rotating plate which ensures that the rotating plate is not pressed against the point where normal force is applied (which would introduce undesired sources of friction). During testing, normal force on the fixture was applied by an Instron machine and lever arm force was applied and measured using a handheld force gauge.

Results of the friction test using Formlabs 3D printed resin are summarized in Table B-1. From the test fixture geometry design, R = 1.1in and l_{arm} = 6in. From these data, the coefficient of friction for the Formlabs resin (against a plastic material) is 0.160 ± 0.023. This value was used

in all models involved 3D printed materials, including with the pushrod concept for the pill release mechanism.

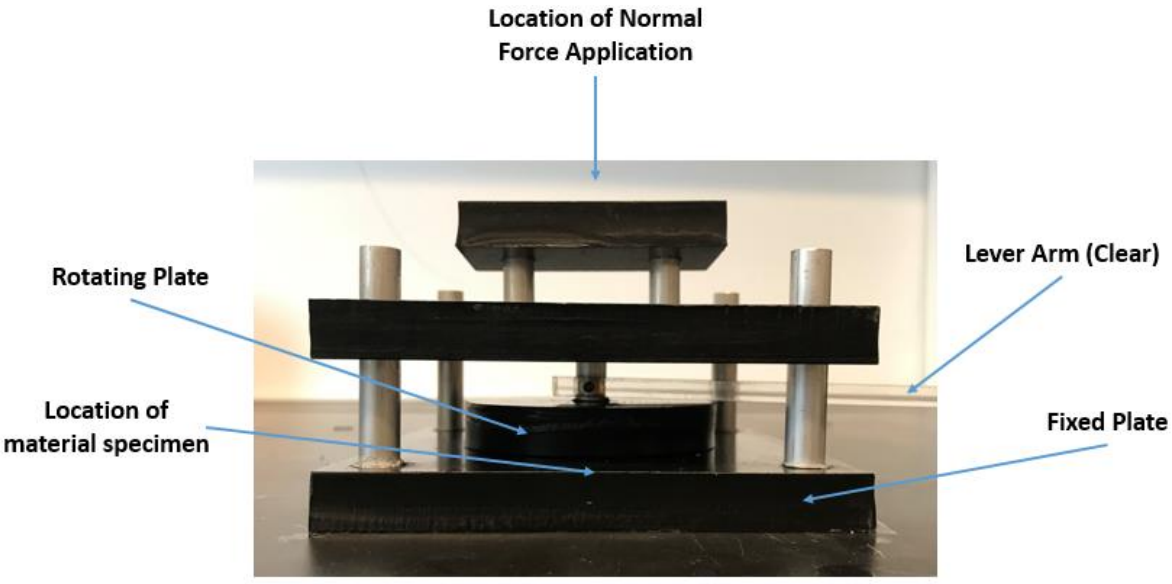

Figure B-2: The test fixture used in friction tests.

Normal Force (N)	200	200	200	200	**Average**
Lever Arm Force (N)	5.0	5.5	7.0	6.0	5.88 ± 0.85
Coefficient of Friction (μ)	0.136	0.150	0.190	0.164	0.160 ± 0.023

Table B-1: Measurements and results from Formlabs 3D printed resin friction test

8. Bibliography

[1] Sabaté, E., and World Health Organization, eds., 2003, *Adherence to Long-Term Therapies: Evidence for Action*, World Health Organization, Geneva.

[2] Tola, H. H., Tol, A., Shojaeizadeh, D., and Garmaroudi, G., 2015, "Tuberculosis Treatment Non-Adherence and Lost to Follow Up among TB Patients with or without HIV in Developing Countries: A Systematic Review," Iran. J. Public Health, **44**(1), pp. 1–11.

[3] Bender, B. G., 2018, "Technology Interventions for Nonadherence: New Approaches to an Old Problem," J. Allergy Clin. Immunol.-Pract., **6**(3), pp. 794–800.

[4] Shiyanbola, O. O., Brown, C. M., and Ward, E. C., 2018, "'I Did Not Want to Take That Medicine': African-Americans' Reasons for Diabetes Medication Nonadherence and Perceived Solutions for Enhancing Adherence," Patient Prefer. Adherence, **12**, pp. 409–421.

[5] Osterberg, L., and Blaschke, T., 2005, "Adherence to Medication," New England Journal of Medicine, **353**(5), pp. 487–497.

[6] Brodtkorb, E., Samsonsen, C., Sund, J. K., Bråthen, G., Helde, G., and Reimers, A., 2016, "Treatment Non-Adherence in Pseudo-Refractory Epilepsy," Epilepsy Res., **122**, pp. 1–6.

[7] Hong, J., Reed, C., Novick, D., Haro, J. M., and Aguado, J., 2011, "Clinical and Economic Consequences of Medication Non-Adherence in the Treatment of Patients with a Manic/Mixed Episode of Bipolar Disorder: Results from the European Mania in Bipolar Longitudinal Evaluation of Medication (EMBLEM) Study," Psychiatry Res, **190**(1), pp. 110–114.

[8] El-Saifi, N., Moyle, W., Jones, C., and Tuffaha, H., 2018, "Medication Adherence in Older Patients With Dementia: A Systematic Literature Review," J. Pharm. Pract., **31**(3), pp. 322–334.

[9] Ventola, C. L., 2015, "The Antibiotic Resistance Crisis," P T, **40**(4), pp. 277–283.

[10] Wang, N., Ma, Y., Liu, Y. H., Du, J., Zhang, H., Xie, S. H., Zhu, K., Lyu, X. Y., Shu, W., Wang, H. H., Zhu, G. F., Tan, S. Y., Fu, Y. Y., Ma, L. P., Zhang, L. Y., Liu, F. Y., Hu, D. Y., Zhang, Y. L., Li, X. Q., and Li, L., 2016, "Risk of Treatment Failure in Patients with Drug-Susceptible Pulmonary Tuberculosis in China," Biomed. Environ. Sci., **29**(8), pp. 612–617.

[11] van Duijn, P. J., Verbrugghe, W., Jorens, P. G., Spöhr, F., Schedler, D., Deja, M., Rothbart, A., Annane, D., Lawrence, C., Nguyen Van, J.-C., Misset, B., Jereb, M., Seme, K., Šifrer, F., Tomiç, V., Estevez, F., Carneiro, J., Harbarth, S., Eijkemans, M. J. C., Bonten, M., and SATURN consortium, 2018, "The Effects of Antibiotic Cycling and Mixing on Antibiotic Resistance in Intensive Care Units: A Cluster-Randomised Crossover Trial," Lancet Infect Dis, **18**(4), pp. 401–409.

[12] Imamovic, L., and Sommer, M. O. A., 2013, "Use of Collateral Sensitivity Networks to Design Drug Cycling Protocols That Avoid Resistance Development," Sci. Transl. Med., **5**(204), p. 204ra132.

[13] Bellinger, A. M., Jafari, M., Grant, T. M., Zhang, S., Slater, H. C., Wenger, E. A., Mo, S., Lee, Y.-A. L., Mazdiyasni, H., Kogan, L., Barman, R., Cleveland, C., Booth, L., Bensel, T., Minahan, D., Hurowitz, H. M., Tai, T., Daily, J., Nikolic, B., Wood, L., Eckhoff, P. A., Langer, R., and Traverso, G., 2016, "Oral, Ultra–Long-Lasting Drug Delivery: Application toward Malaria Elimination Goals," Science Translational Medicine, **8**(365), pp. 365ra157-365ra157.

[14] Vieira, A. L., Oliveira, O., Gomes, M., Gaio, R., and Duarte, R., 2018, “Tuberculosis Incidence Rate among the Homeless Population: The Impact of Socio-Demographic and Health-Related Variables,” Pulmonology.
[15] Sulis, G., Roggi, A., Matteelli, A., and Raviglione, M. C., 2014, “Tuberculosis: Epidemiology and Control,” Mediterr J Hematol Infect Dis, **6**(1).
[16] “WHO | Guidelines for Treatment of Tuberculosis,” WHO [Online]. Available: https://www.who.int/tb/publications/2010/9789241547833/en/. [Accessed: 26-Apr-2019].
[17] Chen, F. J., Dirven, S., Xu, W. L., Bronlund, J., Li, X. N., and Pullan, A., 2012, “Review of the Swallowing System and Process for a Biologically Mimicking Swallowing Robot,” Mechatronics, **22**(5), pp. 556–567.
[18] “Doxycycline Hyclate Oral : Uses, Side Effects, Interactions, Pictures, Warnings & Dosing - WebMD” [Online]. Available: https://www.webmd.com/drugs/2/drug-8648-7073/doxycycline-hyclate-oral/doxycycline-oral/details. [Accessed: 27-Apr-2019].
[19] Verma, M., Vishwanath, K., Eweje, F., Roxhed, N., Grant, T., Castaneda, M., Steiger, C., Mazdiyasni, H., Bensel, T., Minahan, D., Soares, V., Salama, J. A. F., Lopes, A., Hess, K., Cleveland, C., Fulop, D. J., Hayward, A., Collins, J., Tamang, S. M., Hua, T., Ikeanyi, C., Zeidman, G., Mule, E., Boominathan, S., Popova, E., Miller, J. B., Bellinger, A. M., Collins, D., Leibowitz, D., Batra, S., Ahuja, S., Bajiya, M., Batra, S., Sarin, R., Agarwal, U., Khaparde, S. D., Gupta, N. K., Gupta, D., Bhatnagar, A. K., Chopra, K. K., Sharma, N., Khanna, A., Chowdhury, J., Stoner, R., Slocum, A. H., Cima, M. J., Furin, J., Langer, R., and Traverso, G., 2019, “A Gastric Resident Drug Delivery System for Prolonged Gram-Level Dosing of Tuberculosis Treatment,” Science Translational Medicine, **11**(483), p. eaau6267.
[20] Babaee, S., Pajovic, S., Kirtane, A. R., Shi, J., Caffarel-Salvador, E., Hess, K., Collins, J. E., Tamang, S., Wahane, A. V., Hayward, A. M., Mazdiyasni, H., Langer, R., and Traverso, G., 2019, “Temperature-Responsive Biometamaterials for Gastrointestinal Applications,” Science Translational Medicine, **11**(488), p. eaau8581.
[21] Woods, S. P., and Constandinou, T. G., 2013, “Wireless Capsule Endoscope for Targeted Drug Delivery: Mechanics and Design Considerations,” IEEE Transactions on Biomedical Engineering, **60**(4), pp. 945–953.
[22] Munoz, F., Alici, G., and Li, W., 2015, “A Magnetically Actuated Drug Delivery System for Robotic Endoscopic Capsules,” J. Med. Devices, **10**(1), pp. 011004-011004–11.
[23] Dijksman, J. F., Pierik, A., Jongh, F. T. D., Shimizu, J., Zou, H., Albu, L. R., and Weiner, O., 2017, “Modular Ingestible Drug Delivery Capsule.”